Composite Structures 313 (2023) 116900

Contents lists available at ScienceDirect

Composite Structures

journal homepage: www.elsevier.com/locate/compstruct

The mechanics and optimal design of micro-architectured stepped hexagonal lattices

S. Mukherjee [a,*], S. Adhikari [b]

[a] Faculty of Science and Engineering, Swansea University, Bay Campus, Swansea SA1 8EN, UK
[b] James Watt School of Engineering, The University of Glasgow, Glasgow G12 8QQ, UK

ARTICLE INFO

Keywords:
Hexagonal lattices
Stiffness matrix
Elastic properties
Stepped lattices
2D materials

ABSTRACT

This paper conceptualises and analyses a new class of stepped hexagonal lattice achieved through modifying the cross-section of the constituent beams in a controlled manner. The main idea lies in the redistribution of the mass of the constituent beam to obtain a range of equivalent elastic properties, which is not possible within the scope of regular hexagonal lattices. The mass of the stepped lattices is kept the same as the regular hexagonal lattices with equivalent geometry. The in-plane mechanics of such mass-conserved hexagonal lattices are investigated, considering stepped beams as constituent members. The mechanics of a unit cell is exploited to derive the closed-form analytical expressions of equivalent elastic properties of the lattice. The derivation utilises the stiffness elements of the constituent stepped beam members. The stiffness matrices are obtained using two different approaches. They include a semi-analytical condensed stiffness matrix approach based on static substructuring and an analytical method based Castigliano's energy formulation. Both of these approaches are general and can handle arbitrary geometry for the constituent beams. New closed-form analytical expressions of equivalent elastic properties of the lattice are derived. The optimum geometric parameters are obtained by formulating an analytical optimisation problem. It is shown that a unique solution is possible by solving two simultaneous nonlinear equations. The general closed-form expressions of the equivalent elastic properties can be considered benchmark solutions. In the particular case of the regular lattice, they reduce to the well-known classical expressions. Numerical results show that the values of equivalent elastic properties of the lattice can change significantly by redistributing the mass of the constituent beams. It is demonstrated that up to a 37% increase in the equivalent elastic modulus can be achieved compared to the regular lattice by optimally choosing a stepped profile of the constituent elements.

1. Introduction

Mechanical metamaterials are the artificially created engineering structures to achieve the design-specific macro-scale properties [1]. Lattice-based mechanical metamaterials are formed by arranging the periodic unit cell in some particular arrangement to obtain unprecedented effective material properties [2–4]. These cellular structures have a variety of applications in different engineering industries due to their deliverable high stiffness, toughness, energy absorption properties. These materials can be made stiff or flexible depending on the design requirements. The macro-scale properties of the lattice materials are defined by the microstructure of the unit cell and the material properties of the constituent elements. The authors refer to the works of Gibson and Ashby [5] and Fleck et al. [6] for understanding the concept of cellular materials. With the advancement of additive manufacturing, innovative micro-structural design can be exploited [7–10] to explore the fascinating material properties which are not available in nature. Most of the work in literature deals with honeycomb lattices and their applications [11–13]. Researchers also developed generalised homogenisation methods [14–16] to model the mechanical behaviour of hexagonal and heterogeneous lattices [17–21] with different geometries. In this work, we are interested in obtaining a closed-form analytical solution of the mass-conserved hexagonal lattice considering stepped geometry of the constituent beam to explore the wide range of the equivalent elastic properties, which is not achievable with conventional prismatic beam geometry.

Several researchers proposed designs for obtaining a novel class of metamaterials with user-defined properties. The honeycomb material is being studied in an extensive manner [22–29] and utilised to manufacture structural members in the aerospace industry due to their

* Corresponding author S. Mukherjee's Present address: Technical University of Munich, Chair of Vibroacoustics of Vehicles and Machines, 85748 Garching, Germany.
E-mail addresses: shuvajit.mukherjee@gmail.com, shuvajit.mukherjee@tum.de (S. Mukherjee).

https://doi.org/10.1016/j.compstruct.2023.116900
Received 18 September 2022; Received in revised form 18 January 2023; Accepted 5 March 2023
Available online 11 March 2023

high specific stiffness low relative density. The geometric flexibility and manufacturing suitability of the hexagonal material is explored extensively. Researches have been performed to obtain different shapes for the unit cell, such as rectangular, rhombus, re-entrant from the regular hexagonal material. There are studies on analytical prediction of equivalent elastic moduli for regular as well as irregular hexagonal lattices in literature [30–33]. The mechanical properties of the lattice materials are dictated by the material, and geometric properties of the periodic unit cell [34,35]. In this research, we are concerned about the effect of the geometry of the constituent beam members on the material properties of the hexagonal lattice so that a wide range of the material properties can be covered only by redistributing the mass of the constituent beam member. To obtain the material properties, several methods have been explored in the literature. Among them unit cell approach [36–39], energy-based approach [40–45] are well known. All the present works in the literature to obtain the closed-form solution deals with the straight beam members in the unit cell. In this study, the closed-form expression for the hexagonal lattice with stepped geometry for the constituent beam members keeping the mass constant is obtained. To obtain the material properties, the static condensation-based semi-analytical approach and Castigliano's method, along with the unit cell approach, are explored to get the closed-form expressions for the material properties.

This work develops analytical closed-form expressions for the equivalent elastic properties of hexagonal lattices with stepped constituent beam members. The main motivation is to redistribute the mass of a regular straight beam to obtain a large span of the equivalent elastic properties for the lattice to exploit the user-defined design. Previous works deal with multi-material beams and curved beams as the constituent members for the unit cell of the lattice to enhance the design space [46,47] and pave the way for this present study. It is observed that the tailoring of the equivalent material properties can be improved by changing the microstructure of the lattice. Two different methodologies, such as static condensation and Castigliano's method, are utilised to obtain the constituent beam's stiffness matrix. Two geometric parameters, the stepping length ratio (η) and stepping height ratio (α_2), are considered to observe the effect of geometry. These expressions are more general, and the classical homogeneous hexagonal lattice [5] can directly be obtained by considering the limit on some geometric parameters. The formulation can also be utilised for auxetic cases easily. This analysis also considers axial stretching of the constituent elements along with bending. Both Euler–Bernoulli (EB) and Timoshenko beam (TB) theories are considered for analysis. The compact expressions for the beam stiffness where stiffness coefficients are expressed as the same stiffness coefficients of both beam theories multiplied with some geometric coefficients are obtained. One of the major contributions of this study is to find the optimum values of the geometric parameters to obtain the maximum value of the material properties for the mass-conserved lattice. The optimum values are obtained by solving two non-linear simultaneous equations numerically. The results show expanded design space, and the equivalent elastic properties can be varied with a subtle change in those geometric parameters. This generalised approach can be utilised for hexagonal lattice with any kind of geometry for the constituent beam member.

2. The geometry of stepped lattices

2.1. The stepped-up and stepped-down lattices

Fig. 1 shows two types of stepped lattices and their corresponding unit cells. Fig. 1(a) proposes a stepped-up hexagonal lattice with a thicker middle part as illustrated in the unit cell design in Fig. 1(b). On the other hand, Fig. 1(c) proposes a stepped-down hexagonal lattice with two thicker end parts as illustrated in the unit cell design in Fig. 1(d). Such lattices can be fabricated, for example, using additive manufacturing techniques [48,49].

A key aim here is on the derivation of closed-form expression of the equivalent in-plane elastic properties of these two types of stepped hexagonal lattices. The lattices are formed by redistributing the mass of a conventional honeycomb lattice. Our objective is also to investigate the effect of redistribution of mass to obtain a range of equivalent elastic parameter values, which can be exploited for design purposes. In this study, only the stepped configuration is considered. In future, other geometric profile can also be explored in the similar way to obtain some optimal profiles. Due to the mass constraint, the parameters must have some physical limits. The geometry of the constituent beam member of the equivalent regular hexagonal lattice, the stepped lattice and limits on the parameters are described in the next subsection.

2.2. Parameters and their bounds

The parameters for the stepped beam and their bounds are obtained in this section. For the same mass of both regular and stepped beams, the following procedure is developed to obtain two independent parameters and their bounds. The key aim is to equate the mass of the regular beam and the stepped beam. As the out of plane thickness is assumed to be the same for both the beams, the equal-mass requirement effectively translates to having equal surface area. It is assumed that the contribution of material from the joints is negligibly small compared to the overall beam. The values of different lengths and thicknesses in the stepped beam are as follows:

$$L_2 = \eta L \tag{1}$$

$$L_1 = (1 - 2\eta)L \tag{2}$$

$$t_1 = \alpha_1 t \tag{3}$$

$$\text{and} \quad t_2 = \alpha_2 t \tag{4}$$

The total length of the beam is L, and t is the thickness of the equivalent regular beam. For the vertical beam member, the lengths of the different parts can be obtained by replacing L with h in Eqs. (1) and (2). The quantity η is called the *stepping length ratio* and the quantities α_1 and α_2 are called *stepping height ratios*.

Considering the density of the material is ρ, by equating the mass of the regular beam and the stepped beam, one has

$$A\rho = Lt\rho = 2(\alpha_2 t)\eta L\rho + \alpha_1 t(1 - 2\eta)L\rho$$

$$2\alpha_2\eta + \alpha_1(1 - 2\eta) = 1 \tag{5}$$

Therefore, the value of α_1 is obtained as

$$\alpha_1 = \frac{1 - 2\alpha_2\eta}{1 - 2\eta} \tag{6}$$

From a physical point of view, it can be seen that η can only take values $< \frac{1}{2}$. There are two independent geometric parameters stepping height ratio α_2 and stepping length ratio η. To visualise the feasible values of α_1, a contour plot is shown in Fig. 2. It is clear from the plot that for a certain combination of α_2 and η, the value of α_1 becomes negative, which is not physical. Some combination also shows very large values of α_1. The range of values for the parameters should be selected considering the practical feasibility of the geometric dimensions. For that, the values of α_2 and η are chosen in the range of 0.5 to 1.5 and 0.15 to 0.3, respectively.

3. Equivalent elastic properties of stepped lattices

The generalised expressions for the equivalent elastic properties of the stepped lattice will be obtained by analysing the mechanics of a unit cell. The representative example of hexagonal stepped lattices and their corresponding unit cells is shown in Fig. 1. Previous literature showed that the equivalent elastic property of a lattice structure can be obtained by exploiting the periodicity of a suitably selected unit cell. The equivalent elastic property of a lattice structure is obtained

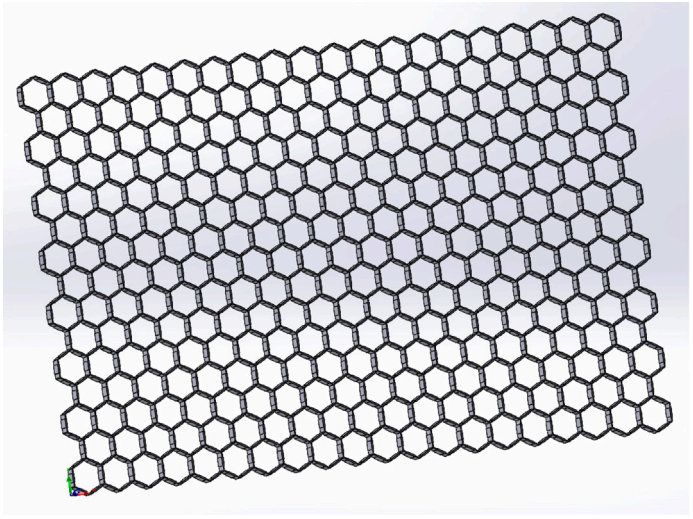

(a) The stepped-up lattice

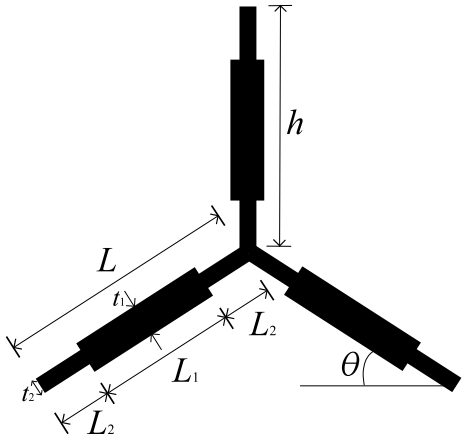

(b) Unit cell: stepped-up lattice

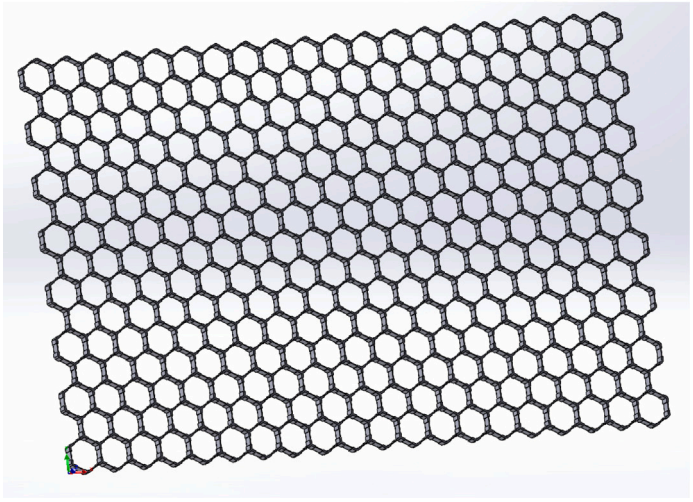

(c) The stepped-down lattice

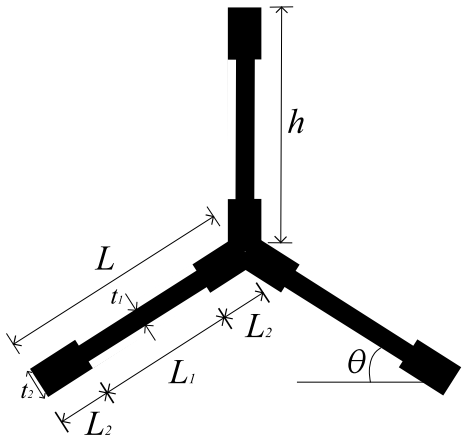

(d) Unit cell: stepped-down lattice

Fig. 1. Schematic diagrams of two proposed stepped lattices and their corresponding unit cells. The key geometric parameters are indicated in the unit-cell of the lattices. The beam has three segments. The length and thickness of the middle segment are L_1 and t_1, respectively. The length and thickness of the two end segments are L_2 and t_2 respectively. The cell angle is denoted as θ.

following the unit cell-based approach. To derive the closed-form expressions for the material properties the stiffness coefficients of the constitutive beam elements were utilised in Ref. [50]. Considering the axial contributions of the beam element, the general matrix expression of the 6×6 symmetric stiffness matrix can be symbolically expressed as

$$\mathbf{K} = \begin{bmatrix} K_{11} & K_{12} & K_{13} & K_{14} & K_{15} & K_{16} \\ K_{21} & K_{22} & K_{23} & K_{24} & K_{25} & K_{26} \\ K_{31} & K_{32} & K_{33} & K_{34} & K_{35} & K_{36} \\ K_{41} & K_{42} & K_{43} & K_{44} & K_{45} & K_{46} \\ K_{51} & K_{52} & K_{53} & K_{54} & K_{55} & K_{56} \\ K_{61} & K_{62} & K_{63} & K_{64} & K_{65} & K_{66} \end{bmatrix} \tag{7}$$

The entries of the stiffness matrix corresponding to for 1 and 4 correspond to the axial deformation and the entries for $2, 3, 5$ and 6 correspond to the bending deformation. In the next subsection, the closed-form expressions are shown as a function of the stiffness coefficients of Eq. (7). Depending upon the beam theory (e.g., Euler–Bernoulli or Timoshenko) and the nature of internal stresses (e.g., tensile or compressive stress), the expressions of the stiffness coefficients will change [51].

3.1. General expressions of equivalent elastic properties

The 2D lattices considered in Fig. 1 in general behave as anisotropic materials with equivalent elastic properties. The key interest of this study is the in-plane elastic properties of the lattices. Five elastic constants govern the homogeneous stress–strain relationship of the 2D material. They include the longitudinal Young's modulus E_1, the transverse Young's modulus E_2, the shear modulus G_{12}, and the Poisson's ratios ν_{12} and ν_{21}. Expressions of these quantities can be obtained considering the mechanics of a unit cell [5]. Analytical expressions of the equivalent elastic properties of 2D lattices were obtained [50] in terms of the element of the stiffness matrix of the constituent beams as given in Eq. (7). The generalised closed-form expressions of the equivalent elastic properties of 2D hexagonal lattices are given as

$$E_1 = \frac{K_{55}\cos\theta}{b(\beta + \sin\theta)\left[\sin^2\theta + \frac{K_{55}}{K_{44}}\cos^2\theta\right]} \tag{8}$$

$$E_2 = \frac{K_{55}(\beta + \sin\theta)}{b\cos^3\theta\left[1 + \tan^2\theta\frac{K_{55}}{K_{44}} + 2\sec^2\theta\frac{K_{55}}{K_{44}^h}\right]} \tag{9}$$

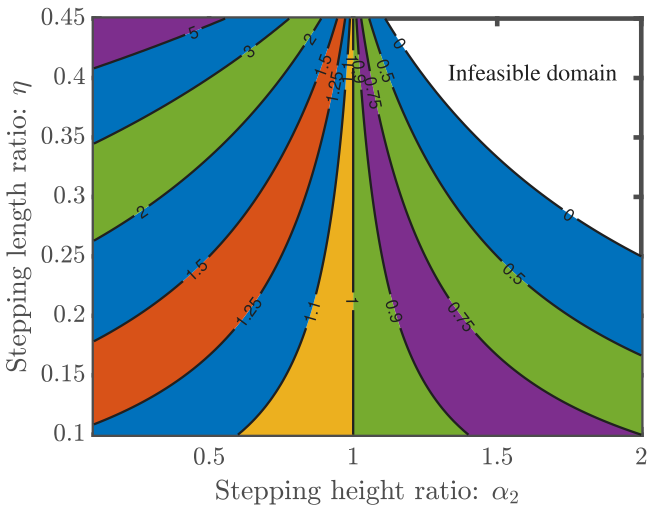

Fig. 2. Contour plot of α_1 as a function of the stepping height ratio α_2 and the stepping length ratio η.

$$\nu_{12} = \frac{\cos^2\theta(1-\frac{K_{55}}{K_{44}})}{(\beta+\sin\theta)\sin\theta(1+\cot^2\theta\frac{K_{55}}{K_{44}})} \tag{10}$$

$$\nu_{21} = \frac{(\beta+\sin\theta)\sin\theta(1-\frac{K_{55}}{K_{44}})}{\left[1+\tan^2\theta\frac{K_{55}}{K_{44}}+2\sec^2\theta\frac{K_{55}}{K_{44}^h}\right]\cos^2\theta} \tag{11}$$

and

$$G_{12} = \frac{1}{\frac{b\cos\theta}{(\beta+\sin\theta)}\left(-\frac{h^2}{2lK_{65}}+\frac{4K_{66}^{(h/2)}}{\left(K_{55}^{(h/2)}K_{66}^{(h/2)}-\left(K_{56}^{(h/2)}\right)^2\right)}\right)+\frac{b\cos\theta}{(\beta+\sin\theta)K_{44}}\left(\cos^2\theta+(\beta+2\sin\theta)\sin\theta\right)+\frac{b\sin\theta}{4\cos\theta K_{44}}\left(4\cos^2\theta+2(\beta+2\sin\theta)\sin\theta\right)} \tag{12}$$

In the above equations, b is the out-of-plane thickness of the constituent beams and the height ratio

$$\beta = \frac{h}{L} \tag{13}$$

The above expressions consider the axial compressing and stretching effect of the beams in addition to the bending effect. The general expressions are valid for any type of constituent beams and any values of θ. When the value of θ is negative, the lattice can show auxetic behaviour (that is, with negative equivalent Poisson's ratios). The equivalent elastic properties require the stiffness coefficients (K_{ij}) of the constituent beam members. This, in turn, requires the stiffness matrix of the constituent stepped beam elements. The stiffness term with superscript h as $(\cdot)^h$ belongs to the stiffness term of the vertical member of the unit cell of the lattice.

The stiffness matrix of the constituent stepped beam elements will be obtained considering two different approaches. Once the stiffness coefficients of the constituent beam members are obtained, they will be substituted in the generalised formula to obtain the equivalent elastic properties of the stepped lattices. In the following subsections, the two approaches are described and the stiffness matrix for both Euler–Bernoulli and Timoshenko beams are derived.

3.2. A semi-analytical sub-structuring based approach

The analytical expressions in Eqs. (8)–(12) are applicable to prismatic beam elements as constituent members of the lattice [24,50]. The same expressions can be utilised for a beam with variable cross-sections or composite cross-sections as the formulae are general. To obtain a more general approach with arbitrary geometries, the idea of static condensation for obtaining the stiffness coefficients of the constituent beam member is utilised. In this approach, the stiffness element components corresponding to only the end degrees of freedom are needed to be considered. This essentially paves the way to utilise the analytical expressions for the effective elastic properties of the entire lattice obtained in [50]. In this work, we are concentrated on stepped constituent beam members, but the idea is valid for any complex beam geometry. The static condensation in the context of the stepped beam is explicitly formulated here. The static equilibrium equation corresponding to the beam element in Fig. 3 can be expressed as

$$\bar{\mathbf{K}}\mathbf{u} = \mathbf{f} \tag{14}$$

where $\bar{\mathbf{K}}$, $\mathbf{f}$ and $\mathbf{u}$ are the stiffness matrix, force vector and the displacement vector, respectively. Note that $\bar{\mathbf{K}}$ is a 12×12 matrix and $\mathbf{f}$ and $\mathbf{u}$ are 12×1 vectors as each node of the beam has three degrees of freedom. Depending on the beam theories the coefficients of the stiffness matrix will change.

Eq. (14) can be partitioned into internal and boundary degrees of freedom. The static equilibrium equation is expressed as

$$\begin{bmatrix}\mathbf{K}_{aa} & \mathbf{K}_{ai}\\ \mathbf{K}_{ia} & \mathbf{K}_{ii}\end{bmatrix}\begin{Bmatrix}\mathbf{u}_a\\ \mathbf{u}_i\end{Bmatrix} = \begin{Bmatrix}\mathbf{f}_a\\ \mathbf{0}\end{Bmatrix} \tag{15}$$

In the above equation, subscript i and a denote the internal and boundary degrees of freedom, respectively. For the stepped beam mentioned in Fig. 3 there are three elements and four nodes and 12 degrees of freedom. the internal degrees of freedom are 4–9 and the boundary degrees of freedom are 1, 2, 3, 10, 11, and 12. The condensed equation of equilibrium can be obtained by eliminating the internal degrees of freedom as

$$\underbrace{\left(\mathbf{K}_{aa}-\mathbf{K}_{ai}\mathbf{K}_{ii}^{-1}\mathbf{K}_{ia}\right)}_{\mathbf{K}}\mathbf{u}_a = \mathbf{f}_a \tag{16}$$

The above equation is expressed in terms of the boundary degrees of freedom and is equivalent to the original equilibrium equation. The condensed stiffness matrix $\mathbf{K}$ in Eq. (16) has a dimension of 6×6, as in Eq. (7). The elements of the condensed stiffness matrix can be utilised in the analytical expressions for obtaining the equivalent elastic moduli and Poisson's ratio of the lattices with general constituent beam elements. Further, the above approach can account for the effect of spatially varying geometric and material properties within the constituent beam element. This approach is termed semi-analytical because the closed-form expressions obtained by symbolic operations are large, and complex beam geometries can further complicate the expressions. In this work, we consider three beam elements as described in Fig. 3(a). The flexibility of this approach lies in the exploitation of the finite element method to obtain the condensed stiffness matrix and then utilisation of the required stiffness terms for calculating the equivalent elastic properties of the lattice. In effect, this is a multi-scale approach where microscopic finite element analysis is unified with macroscopic homogenised equivalent elastic properties. In the next section, we propose the Castigliano based approach to obtain the stiffness matrix of the constituent beam member. Subsequently, the stiffness terms are used to obtain the closed-form expressions for the equivalent elastic moduli of the entire lattice material.

3.3. The Castigliano's approach

In this section, the procedure to obtain the stiffness matrix of the constituent stepped beam member is proposed. Castigliano's method is utilised to derive the exact stiffness matrix [52,53]. To explain the essential equations of Castigliano's approach, the generalised force and displacements are shown in Fig. 4. To obtain the stiffness matrix,

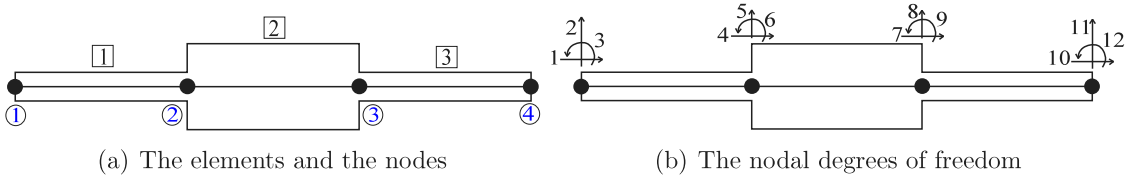

(a) The elements and the nodes (b) The nodal degrees of freedom

Fig. 3. Finite element modelling of a stepped beam. There are three beam elements and four nodes. Each node has three degrees of freedom. This results into a 12 degrees of freedom model for the analysis.

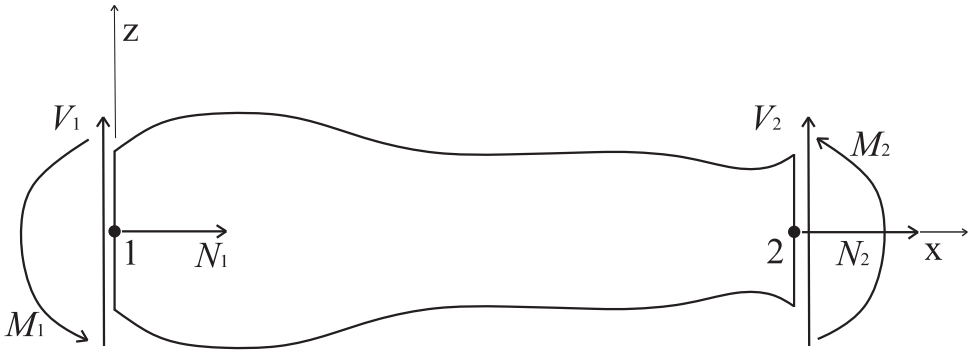

Fig. 4. Schematic diagram of a general two-noded beam member with a variable cross-section. The quantities V_1, M_1 and N_1 are the shear force, bending moments and axial forces, respectively at node 1. The quantities V_2, M_2 and N_2 are the shear force, bending moments and axial forces, respectively at node 2.

a flexibility-based approach is considered. The matrix form of the force–displacement relation for a general beam can be expressed as

$$\mathbf{v}^b = \mathbf{K}^b\mathbf{u}^b \tag{17}$$

Here $\mathbf{v}^b$ and $\mathbf{u}^b$ are the generalised force and displacement vectors of the following form

$$\mathbf{v}^b = \{V_1, M_1, V_2, M_2\}^T \tag{18}$$

$$\text{and} \quad \mathbf{u}^b = \{w_1, \theta_1, w_2, \theta_2\}^T \tag{19}$$

and $\mathbf{K}^b$ is the 4×4 stiffness matrix. The superscript b stands for the contribution from the bending part of the beam. w_i and θ_i $(i = 1, 2)$ are the nodal bending displacements and rotations of the beam cross-section, respectively. To obtain the stiffness coefficients, the flexibility approach is considered followed by the equilibrium conditions. To derive the force–displacement relationship for node 1, node 2 is kept fixed (all three degrees of freedom are restrained) and generalised forces N_1, V_1 and M_1 are applied on node 1.

Both axial and bending deflections are considered in the formulation. So, the strain energy has both axial and bending contributions as follows

$$U = \frac{1}{2}\int_0^L \frac{M^2}{EI(x)}dx + \frac{1}{2}\int_0^L \frac{N^2}{EA(x)}dx \tag{20}$$

The flexibility matrix of the axial and bending part are determined separately. The internal moment and forces are $M = V_1 x - M_1$ and $N = N_1$. The flexibility relationship of the beam considering the bending part is given by

$$\begin{Bmatrix} w_1 \\ \theta_1 \end{Bmatrix} = \begin{Bmatrix} \dfrac{\partial U}{\partial V_1} \\ \dfrac{\partial U}{\partial M_1} \end{Bmatrix} = \begin{bmatrix} Q_3 & -Q_2 \\ -Q_2 & Q_1 \end{bmatrix} \begin{Bmatrix} V_1 \\ M_1 \end{Bmatrix} \tag{21}$$

The coefficients Q_is are defined as

$$Q_i = \int_0^L \frac{x^{(i-1)}}{EI(x)}dx, \qquad i = 1, 2, 3 \tag{22}$$

The stiffness relationship can be found by inverting the flexibility Eq. (21) as

$$\begin{Bmatrix} V_1 \\ M_1 \end{Bmatrix} = \frac{1}{D_1}\begin{bmatrix} Q_1 & Q_2 \\ Q_2 & Q_3 \end{bmatrix} \begin{Bmatrix} w_1 \\ \theta_1 \end{Bmatrix} \tag{23}$$

where, $D_1 = Q_1Q_3 - Q_2^2$. In a similar way, the direct flexibility matrix for point 2 can be obtained. For that, we have to fix point 1 and apply Castigliano's 2nd theorem after putting the internal moment equation $M = V_2(L - x) - M_2$ in Eq. (20)

$$\begin{Bmatrix} w_2 \\ \theta_2 \end{Bmatrix} = \begin{Bmatrix} \dfrac{\partial U}{\partial V_1} \\ \dfrac{\partial U}{\partial M_1} \end{Bmatrix} = \begin{bmatrix} R_3 & -R_2 \\ -R_2 & R_1 \end{bmatrix} \begin{Bmatrix} V_2 \\ M_2 \end{Bmatrix} \tag{24}$$

Here R_is are given by

$$R_i = \int_0^L \frac{(L - x)^{(i-1)}}{EI(x)}dx, \qquad i = 1, 2, 3 \tag{25}$$

The stiffness relationship for node 2 can be found by inverting the flexibility relation Eq. (24) as

$$\begin{Bmatrix} V_2 \\ M_2 \end{Bmatrix} = \frac{1}{D_2}\begin{bmatrix} R_1 & R_2 \\ R_2 & R_3 \end{bmatrix} \begin{Bmatrix} w_2 \\ \theta_2 \end{Bmatrix} \tag{26}$$

where, $D_2 = R_1R_3 - R_2^2$. The stiffness terms corresponding to the coupling between nodes 1 and 2 can be found considering the moment and force equilibrium. For the force equilibrium one obtains $V_1 = -V_2$ and for the moment equilibrium we have $M_1 + M_2 + V_2L = 0$. These two equilibrium conditions eventually give

$$\mathbf{K}^b_{1i} = -\mathbf{K}^b_{3i}, \qquad i = 1, \ldots, 4 \tag{27}$$

$$\text{and} \quad \mathbf{K}^b_{24} = -(\mathbf{K}^b_{44} + \mathbf{K}^b_{34}L) \tag{28}$$

The complete bending stiffness matrix is obtained by substituting Eqs. (23), (26), (27), and (28) into Eq. (17). After some simplifications, the 4×4 bending stiffness matrix can be expressed considering the three

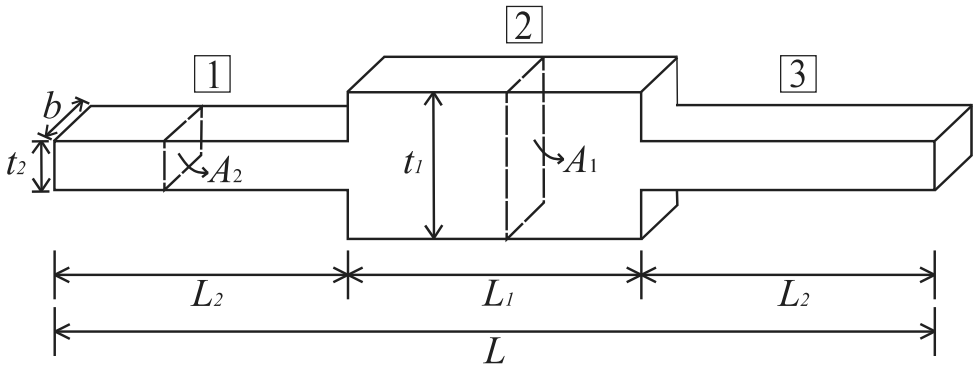

Fig. 5. Schematic diagram of a stepped beam with geometric details. The beam has three parts. The length, thickness and area of middle segment are L_1, t_1, and A_1 respectively. The length, thickness and area of the two end segments are L_2, t_2, and A_2 respectively. The width of the beam is b.

independent coefficients in Eq. (22) as

$$\mathbf{K}^b = \frac{1}{D_1}\begin{bmatrix} Q_1 & Q_2 & -Q_1 & (Q_1L - Q_2) \\ Q_2 & Q_3 & -Q_3 & (Q_2L - Q_3) \\ -Q_1 & -Q_2 & Q_1 & -(Q_1L - Q_2) \\ (Q_1L - Q_2) & (Q_2L - Q_3) & -(Q_1L - Q_2) & (Q_1L^2 - 2Q_2L + Q_3) \end{bmatrix} \tag{29}$$

Now we turn our attention to the stiffness matrix corresponding to the axial deformation. Following a similar procedure, the 2×2 axial stiffness matrix is given by

$$\mathbf{K}^a = \frac{1}{S}\begin{bmatrix} 1 & -1 \\ -1 & 1 \end{bmatrix} \tag{30}$$

where the integral

$$S = \int_0^L \frac{1}{EA(x)}dx \tag{31}$$

The expressions of the bending and axial stiffness matrices are general and involve the evaluations of respective integrals. The full 6×6 stiffness matrix can be obtained by using the elements of these matrices in the respective degrees of freedom as shown in Fig. 4. Next, two special cases for the application of this general formulation is considered.

3.3.1. Considering Euler–Bernoulli beam assumption

We consider a stepped beam and the domain is divided into three parts as shown in Fig. 5. The variable bending stiffness $EI(x)$, therefore, takes the form of

$$EI(x) = \begin{cases} EI_2 & 0 \le x < L_2 \\ EI_1 & L_2 \le x < L_2 + L_1 \\ EI_2 & L_2 + L_1 \le x < L \end{cases} \tag{32}$$

where $I_1 = bt_1^3/12$ and $I_2 = bt_2^3/12$. For the derivation of the axial stiffness matrix, it is noted that

$$EA(x) = \begin{cases} EA_2 & 0 \le x < L_2 \\ EA_1 & L_2 \le x < L_2 + L_1 \\ EA_2 & L_2 + L_1 \le x < L \end{cases} \tag{33}$$

where $A_1 = bt_1$ and $A_2 = bt_2$.

Using these expressions of $EI(x)$ and $EA(x)$, the equation for the strain energy becomes

$$U = \frac{1}{2}\int_0^{L_2} \frac{M^2}{EI_2}dx + \frac{1}{2}\int_0^{L_2} \frac{N^2}{EA_2}dx + \frac{1}{2}\int_{L_1}^{L_1+L_2} \frac{M^2}{EI_1}dx + \frac{1}{2}\int_{L_1}^{L_1+L_2} \frac{N^2}{EA_1}dx + \frac{1}{2}\int_{L_1+L_2}^{L} \frac{M^2}{EI_2}dx + \frac{1}{2}\int_{L_1+L_2}^{L} \frac{N^2}{EA_2}dx \tag{34}$$

The coefficients Q_is for the stepped beam are defined as

$$Q_i = \int_0^{L_2} \frac{x^{(i-1)}}{EI_2}dx + \int_{L_2}^{L_1+L_2} \frac{x^{(i-1)}}{EI_1}dx + \int_{L_1+L_2}^{L} \frac{x^{(i-1)}}{EI_2}dx, \qquad i = 1, 2, 3 \tag{35}$$

For the axial stiffness matrix we have

$$S = \int_0^{L_1} \frac{1}{EA_2}dx + \int_{L_1}^{L_1+L_2} \frac{1}{EA_1}dx + \int_{L_1+L_2}^{L} \frac{1}{EA_2}dx \tag{36}$$

The stiffness contributions for the bending and axial parts are obtained separately. After performing the symbolic operations and algebraic simplifications we obtained the stiffness matrix for the constituent stepped Euler–Bernoulli beam as

$$\mathbf{K} = \begin{bmatrix} a_1\frac{EA}{L} & 0 & 0 & -a_1\frac{EA}{L} & 0 & 0 \\ 0 & d_1\frac{12EI}{L^3} & d_2\frac{6EI}{L^2} & 0 & -d_1\frac{12EI}{L^3} & d_2\frac{6EI}{L^2} \\ 0 & d_2\frac{6EI}{L^2} & d_3\frac{4EI}{L} & 0 & -d_2\frac{6EI}{L^2} & d_4\frac{2EI}{L} \\ -a_1\frac{EA}{L} & 0 & 0 & a_1\frac{EA}{L} & 0 & 0 \\ 0 & -d_1\frac{12EI}{L^3} & -d_2\frac{6EI}{L^2} & 0 & d_1\frac{12EI}{L^3} & -d_2\frac{6EI}{L^2} \\ 0 & d_2\frac{6EI}{L^2} & d_4\frac{2EI}{L} & 0 & -d_2\frac{6EI}{L^2} & d_3\frac{4EI}{L} \end{bmatrix} \tag{37}$$

Here A and I are the cross-sectional area and moment of inertia of the regular beam with same mass as the stepped beam, that is

$$I = \frac{1}{12}bt^3 \quad \text{and} \quad A = bt \tag{38}$$

The scalar coefficients appearing in Eq. (37) are derived as

$$a_1 = \frac{1}{\alpha_1^2 - 2\eta(\alpha_1^2 - \alpha_2^2)} \tag{39}$$

$$d_1 = \frac{\alpha_1^3\alpha_2^3}{(\alpha_1^3 - \alpha_2^3)\left((2\eta - 1)^3 + 1\right) + \alpha_2^3} \tag{40}$$

$$d_2 = d_1 \tag{41}$$

$$d_3 = \frac{\alpha_1^3\alpha_2^3\left((\alpha_1^3 - \alpha_2^3)((\eta - 1)^3 + 1 + \eta^3) + \alpha_2^3\right)}{\left(2\eta(\alpha_1^3 - \alpha_2^3) + \alpha_2^3\right)\left((\alpha_1^3 - \alpha_2^3)\left((2\eta - 1)^3 + 1\right) + \alpha_2^3\right)} \tag{42}$$

$$\text{and} \quad d_4 = \frac{\alpha_1^3\alpha_2^3\left(\alpha_2^3 - (\alpha_1^3 - \alpha_2^3)(4\eta^3 - 6\eta^2)\right)}{\left(2\eta(\alpha_1^3 - \alpha_2^3) + \alpha_2^3\right)\left((\alpha_1^3 - \alpha_2^3)\left((2\eta - 1)^3 + 1\right) + \alpha_2^3\right)} \tag{43}$$

These coefficients are highly nonlinear functions of only the geometric parameters (stepping length ratio and stepping height ratios) of the

stepped beam. Eq. (37), along with the definition of these coefficients gives the exact stiffness matrix of the stepped beam in Fig. 4 in closed-form using the Euler–Bernoulli beam assumption.

The case of a conventional regular prismatic beam appears when we take the limits $\lim_{\alpha_1\to1,\alpha_2\to1}$ in the expressions derived in Eqs. (39)–(43). Taking the mathematical limits, the coefficients a_1 and d_i become

$$\lim_{\alpha_1\to1,\alpha_2\to1} a_1 = \lim_{\alpha_1\to1,\alpha_2\to1} \frac{1}{\alpha_1^2-2\eta(\alpha_1^2-\alpha_2^2)} = 1 \tag{44}$$

$$\lim_{\alpha_1\to1,\alpha_2\to1} d_1 = \lim_{\alpha_1\to1,\alpha_2\to1} \frac{\alpha_1^3\alpha_2^3}{(\alpha_1^3-\alpha_2^3)\left((2\eta-1)^3+1\right)+\alpha_2^3} = 1 \tag{45}$$

$$d_2 = 1 \tag{46}$$

$$\lim_{\alpha_1\to1,\alpha_2\to1} d_3 = \lim_{\alpha_1\to1,\alpha_2\to1} \frac{\alpha_1^3\alpha_2^3\left((\alpha_1^3-\alpha_2^3)((\eta-1)^3+1+\eta^3)+\alpha_2^3\right)}{\left(2\eta(\alpha_1^3-\alpha_2^3)+\alpha_2^3\right)\left((\alpha_1^3-\alpha_2^3)\left((2\eta-1)^3+1\right)+\alpha_2^3\right)} = 1 \tag{47}$$

$$\lim_{\alpha_1\to1,\alpha_2\to1} d_4 = \lim_{\alpha_1\to1,\alpha_2\to1} \frac{\alpha_1^3\alpha_2^3\left(\alpha_2^3-(\alpha_1^3-\alpha_2^3)(4\eta^3-6\eta^2)\right)}{\left(2\eta(\alpha_1^3-\alpha_2^3)+\alpha_2^3\right)\left((\alpha_1^3-\alpha_2^3)\left((2\eta-1)^3+1\right)+\alpha_2^3\right)} = 1 \tag{48}$$

Considering these limiting values, we get the stiffness matrix for the regular Euler–Bernoulli beam as

$$\mathbf{K} = \begin{bmatrix} \frac{EA}{L} & 0 & 0 & -\frac{EA}{L} & 0 & 0 \\ 0 & \frac{12EI}{L^3} & \frac{6EI}{L^2} & 0 & -\frac{12EI}{L^3} & \frac{6EI}{L^2} \\ 0 & \frac{6EI}{L^2} & \frac{4EI}{L} & 0 & -\frac{6EI}{L^2} & \frac{2EI}{L} \\ -\frac{EA}{L} & 0 & 0 & \frac{EA}{L} & 0 & 0 \\ 0 & -\frac{12EI}{L^3} & -\frac{6EI}{L^2} & 0 & \frac{12EI}{L^3} & -\frac{6EI}{L^2} \\ 0 & \frac{6EI}{L^2} & \frac{2EI}{L} & 0 & -\frac{6EI}{L^2} & \frac{4EI}{L} \end{bmatrix} \tag{49}$$

This expression match exactly with the well known expression for Euler–Bernoulli beam [54]. This analysis shows that the expressions derived in Eq. (37) are the generalisation of the classical expression of the regular beam to the stepped beam.

3.3.2. Considering Timoshenko beam assumption

In this section, the stiffness matrix for the stepped beam is obtained considering the Timoshenko beam assumption. In the case of the Timoshenko beam, there is one extra term in the strain energy from the shear contribution. The strain energy of the beam becomes

$$U = \frac{1}{2}\int_0^L \frac{M^2}{EI(x)}dx + \frac{1}{2}\int_0^L \frac{V^2}{kGA(x)}dx + \frac{1}{2}\int_0^L \frac{N^2}{EA(x)}dx \tag{50}$$

The bending stiffness $EI(x)$ and the axial stiffness $EA(x)$ for three parts of the beam are already mentioned in Eqs. (32) and (33), respectively. Similarly, the shear stiffness is expressed as

$$kGA(x) = \begin{cases} kGA_2 & 0 \le x < L_2 \\ kGA_1 & L_2 \le x < L_2+L_1 \\ kGA_2 & L_2+L_1 \le x < L \end{cases} \tag{51}$$

In the above equation, k is the shear coefficient snd G is the shear modulus of the beam material. The total strain energy is

$$\begin{aligned} U = {} & \frac{1}{2}\int_0^{L_2} \frac{M^2}{EI_2}dx + \frac{1}{2}\int_0^{L_2} \frac{N^2}{EA_2}dx + \frac{1}{2}\int_0^{L_2} \frac{V^2}{kGA_2}dx \\ & + \frac{1}{2}\int_{L_1}^{L_1+L_2} \frac{M^2}{EI_1}dx + \frac{1}{2}\int_{L_1}^{L_1+L_2} \frac{N^2}{EA_1}dx + \frac{1}{2}\int_{L_1}^{L_1+L_2} \frac{V^2}{kGA_1}dx \\ & + \frac{1}{2}\int_{L_1+L_2}^{L} \frac{M^2}{EI_2}dx + \frac{1}{2}\int_{L_1+L_2}^{L} \frac{N^2}{EA_2}dx + \frac{1}{2}\int_{L_1+L_2}^{L} \frac{V^2}{kGA_2}dx \end{aligned} \tag{52}$$

The internal moment, shear and forces are $M = V_1x - M_1$, $V = V_1$ and $N = N_1$. The expressions for the flexibility relation, stiffness relation of the beam are same as Eq. (21) and Eq. (23). Whereas, the coefficients Q_is are as follows

$$Q_i = \int_0^{L_2} \frac{x^{(i-1)}}{EI_2}dx + \int_{L_2}^{L_1+L_2} \frac{x^{(i-1)}}{EI_1}dx + \int_{L_1+L_2}^{L} \frac{x^{(i-1)}}{EI_2}dx, \qquad i = 1,2 \tag{53}$$

and

$$Q_3 = \int_0^{L_2} \frac{x^2}{EI_2}dx + \int_0^{L_2} \frac{1}{kGA_2}dx + \int_{L_2}^{L_1+L_2} \frac{x^2}{EI_1}dx \tag{54}$$

$$+ \int_{L_2}^{L_1+L_2} \frac{1}{kGA_1}dx + \int_{L_1+L_2}^{L} \frac{x^2}{EI_2}dx + \int_{L_1+L_2}^{L} \frac{1}{kGA_2}dx \tag{55}$$

The axial stiffness matrix components will be the same as Eq. (37) as it is not affected by the Timoshenko beam assumption. The stiffness contributions for the bending and axial parts are obtained separately. After performing the symbolic operations and algebraic simplifications we obtained the stiffness matrix for the constituent Timoshenko beam as

$$\mathbf{K} = \begin{bmatrix} a_1\frac{EA}{L} & 0 & 0 & -a_1\frac{EA}{L} & 0 & 0 \\ 0 & \bar{d}_1\frac{12EI}{L^3} & \bar{d}_2\frac{6EI}{L^2} & 0 & -\bar{d}_1\frac{12EI}{L^3} & \bar{d}_2\frac{6EI}{L^2} \\ 0 & \bar{d}_2\frac{6EI}{L^2} & \bar{d}_3\frac{4EI}{L} & 0 & -\bar{d}_2\frac{6EI}{L^2} & \bar{d}_4\frac{2EI}{L} \\ -a_1\frac{EA}{L} & 0 & 0 & a_1\frac{EA}{L} & 0 & 0 \\ 0 & -\bar{d}_1\frac{12EI}{L^3} & -\bar{d}_2\frac{6EI}{L^2} & 0 & \bar{d}_1\frac{12EI}{L^3} & -\bar{d}_2\frac{6EI}{L^2} \\ 0 & \bar{d}_2\frac{6EI}{L^2} & \bar{d}_4\frac{2EI}{L} & 0 & -\bar{d}_2\frac{6EI}{L^2} & \bar{d}_3\frac{4EI}{L} \end{bmatrix} \tag{56}$$

with

$$a_1 = \frac{1}{\alpha_1^2-2\eta(\alpha_1^2-\alpha_2^2)} \tag{57}$$

$$\bar{d}_1 = \frac{\alpha_1^3\alpha_2^3(2\eta\alpha_1^3-2\eta\alpha_2^3+\alpha_2^3)}{\bar{D}_1} \tag{58}$$

$$\bar{d}_2 = \bar{d}_1 \tag{59}$$

$$\bar{d}_3 = \frac{\alpha_1^3\alpha_2^3\left(\alpha_2^3(4+\Phi\alpha_1^2)+4(\alpha_1^3-\alpha_2^3)(2\eta^3-3\eta^2+3\eta)+2\eta\Phi\alpha_1^2\alpha_2^2(\alpha_1-\alpha_2)\right)}{\bar{D}_1} \tag{60}$$

$$\bar{d}_4 = \frac{\alpha_1^3\alpha_2^3(6(\alpha_2^3+2\eta(\alpha_1^3-\alpha_2^3))-4(\alpha_2^3+(\alpha_1^3-\alpha_2^3)(2\eta^3-3\eta^2+3\eta)))-\Phi\alpha_1^5\alpha_2^5(2\eta(\alpha_1-\alpha_2)+\alpha_2)}{\bar{D}_1} \tag{61}$$

and

$$\bar{D}_1 = (\alpha_2^3+2\eta(\alpha_1^3-\alpha_2^3))(\alpha_1^3+\Phi\alpha_1^2\alpha_2^2(\alpha_2+2\eta(\alpha_1-\alpha_2))-(1-2\eta)^3(\alpha_1^3-\alpha_2^3)) \tag{62}$$

If we take the limit $\lim_{\alpha_1\to1,\alpha_2\to1}$ (the case of a regular beam), then the coefficients a_1 and $\bar{d}_i$ become

$$\lim_{\alpha_1\to1,\alpha_2\to1} a_1 = \lim_{\alpha_1\to1,\alpha_2\to1} \frac{1}{\alpha_1^2-2\eta(\alpha_1^2-\alpha_2^2)} = 1 \tag{63}$$

$$\lim_{\alpha_1\to1,\alpha_2\to1} \bar{d}_1 = \lim_{\alpha_1\to1,\alpha_2\to1} \frac{\alpha_1^3\alpha_2^3(2\eta\alpha_1^3-2\eta\alpha_2^3+\alpha_2^3)}{\bar{D}_1} = \frac{1}{1+\Phi} \tag{64}$$

$$\bar{d}_2 = \bar{d}_1 \tag{65}$$

$$\lim_{\alpha_1\to1,\alpha_2\to1} \bar{d}_3 = \lim_{\alpha_1\to1,\alpha_2\to1} \frac{\alpha_1^3\alpha_2^3\left(\alpha_2^3(4+\Phi\alpha_1^2)+4(\alpha_1^3-\alpha_2^3)(2\eta^3-3\eta^2+3\eta)+2\eta\Phi\alpha_1^2\alpha_2^2(\alpha_1-\alpha_2)\right)}{\bar{D}_1} = \frac{4+\Phi}{1+\Phi} \tag{66}$$

$$\lim_{\alpha_1\to 1,\alpha_2\to 1} \bar{d}_4 = \lim_{\alpha_1\to 1,\alpha_2\to 1} \frac{\alpha_1^3\alpha_2^3(6(\alpha_2^3+2\eta(\alpha_1^3-\alpha_2^3))-4(\alpha_2^3+(\alpha_1^3-\alpha_2^3)(2\eta^3-3\eta^2+3\eta)))}{\bar{D}_1} - \frac{\Phi\alpha_1^5\alpha_2^5(2\eta(\alpha_1-\alpha_2)+\alpha_2)}{\bar{D}_1} = \frac{2-\Phi}{1+\Phi} \tag{67}$$

Considering these limiting values in Eq. (56), one obtains the stiffness matrix for the regular Timoshenko beam as

$$\mathbf{K} = \begin{bmatrix} \frac{EA}{L} & 0 & 0 & -\frac{EA}{L} & 0 & 0 \\ 0 & 12\frac{EI}{(1+\Phi)L^3} & 6\frac{EI}{(1+\Phi)L^2} & 0 & -12\frac{EI}{(1+\Phi)L^3} & 6\frac{EI}{(1+\Phi)L^2} \\ 0 & 6\frac{EI}{(1+\Phi)L^2} & \frac{(4+\Phi)EI}{(1+\Phi)L} & 0 & -6\frac{EI}{(1+\Phi)L^2} & \frac{(2-\Phi)EI}{(1+\Phi)L} \\ -\frac{EA}{L} & 0 & 0 & \frac{EA}{L} & 0 & 0 \\ 0 & 12\frac{EI}{(1+\Phi)L^3} & -6\frac{EI}{(1+\Phi)L^2} & 0 & 12\frac{EI}{(1+\Phi)L^3} & -6\frac{EI}{(1+\Phi)L^2} \\ 0 & 6\frac{EI}{(1+\Phi)L^2} & \frac{(2-\Phi)EI}{(1+\Phi)L} & 0 & -6\frac{EI}{(1+\Phi)L^2} & \frac{(4+\Phi)EI}{(1+\Phi)L} \end{bmatrix} \tag{68}$$

The expression of the stiffness matrix for the Timoshenko beam in Eq. (68) matches exactly will the well-known expression [54]. The expressions derived in Eq. (56) is the generalisation of the classical expression of the regular beam to the stepped beam.

The term Φ gives the relative importance of the shear deformations to the bending deformations. For the equivalent rectangular cross-section

$$\Phi = \frac{12EI}{kAGL^2} = \frac{2(1+\nu)}{k}\left(\frac{t}{L}\right)^2 \tag{69}$$

Here is ν is the Poisson's ratio of the beam material, $I = bt^3/12$, $A = bt$. We have used the relationships

$$G = \frac{E}{2(1+\nu)} \tag{70}$$

The generalised expression of the stepped Timoshenko beam given in Eq. (56) reduces to stiffness matrix for the stepped Euler–Bernoulli beam in (37) for $\Phi = 0$. Consequently, the expression of the regular Timoshenko beam stiffness matrix in (68) reduces to the classical Euler–Bernoulli case in Eq. (49) for $\Phi = 0$. The expression of the stiffness matrix in Eq. (56) is, therefore, the most general expression derived in this paper.

3.4. Closed-form expressions of equivalent elastic moduli

In this subsection, the analytical expressions derived before are utilised to develop explicit closed-form expressions of equivalent elastic moduli of the stepped lattice.

3.4.1. Equivalent elastic moduli with Euler–Bernoulli beam theory

We consider the stiffness coefficients from Eq. (37) and define the thickness ratio as

$$\alpha = \frac{t}{L} \tag{71}$$

Here t is the thickness of the regular straight beam. From the expressions (8)–(12), it can be observed that two coefficients of the 6×6 element stiffness matrix of the inclined member and one coefficients of the 6×6 element stiffness matrix of vertical member, namely, K_{55}, K_{44} and $K_{44}^{(h)}$, are necessary to obtain the equivalent elastic properties of the lattice. Using the expressions of the moment of inertia and the cross-sectional area, the stiffness coefficients are given by

$$K_{55} = d_1\frac{12EI}{L^3} = d_1Eb\alpha^3, K_{44} = a_1\frac{EA}{L} = a_1Eb\alpha \quad \text{and} \quad K_{44}^{(h)} = a_1\frac{EA}{h} = a_1\frac{Eb\alpha}{\beta} \tag{72}$$

Also,

$$\frac{K_{55}}{K_{44}} = \alpha^2\frac{d_1}{a_1} \quad \text{and} \quad \frac{K_{55}}{K_{44}^h} = \alpha^2\beta\frac{d_1}{a_1} \tag{73}$$

Here, I is the moment of inertia for the equivalent regular beam.

The generalised expressions for the stepped lattice are explicitly obtained as

$$E_1 = \frac{d_1E\alpha^3\cos\theta}{(\beta+\sin\theta)\left(\sin^2\theta+\alpha^2\frac{d_1}{a_1}\cos^2\theta\right)} \tag{74}$$

$$E_2 = \frac{d_1E\alpha^3(\beta+\sin\theta)}{\cos^3\theta\left(1+\alpha^2\frac{d_1}{a_1}\tan^2\theta+2\alpha^2\beta\frac{d_1}{a_1}\sec^2\theta\right)} \tag{75}$$

$$\nu_{12} = \frac{\left(1-\alpha^2\frac{d_1}{a_1}\right)\sin\theta\cos^2\theta}{(\beta+\sin\theta)\left(\sin^2\theta+\alpha^2\frac{d_1}{a_1}\cos^2\theta\right)} \tag{76}$$

$$\text{and} \quad \nu_{21} = \frac{(1-\alpha^2\frac{d_1}{a_1})\sin\theta(\beta+\sin\theta)}{\left(1+\alpha^2\frac{d_1}{a_1}\tan^2\theta+2\alpha^2\beta\frac{d_1}{a_1}\sec^2\theta\right)\cos^2\theta} \tag{77}$$

The generalised expression of the shear modulus (Eq. (12)) consists of five stiffness coefficients from the two constituent beam members. There are the two coefficients, $K_{65} = -6EId_2/L^2$ and $K_{44} = EAa_1/L$ from the inclined members and three coefficients from the verticle member. The coefficients from the vertical member are

$$K_{55}^{h/2} = \frac{12EI}{(h/2)^3}d_{1h} \tag{78}$$

$$K_{56}^{h/2} = -\frac{6EI}{(h/2)^2}d_{2h} \tag{79}$$

$$\text{and} \quad K_{66}^{h/2} = \frac{4EI}{(h/2)}d_{3h} \tag{80}$$

The closed-form equation for the shear modulus is obtained by substituting the expressions of the stiffness coefficients in Eq. (12) as

$$G_{12} = \frac{E\alpha^3\cos\theta\,(\beta+\sin\theta)\,a_1d_2\left(4d_{1h}d_{3h}-3{d_{2h}}^2\right)}{\left(2a_1d_2\beta+\left(a_1-\alpha^2d_2\right)\left(4d_{1h}d_{3h}-3{d_{2h}}^2\right)\right)\beta^2\cos^2\theta + d_2\alpha^2\left(1+2\beta\sin\theta+\beta^2\right)\left(4d_{1h}d_{3h}-3{d_{2h}}^2\right)} \tag{81}$$

where,

$$d_{1h} = \frac{\alpha_1^3\alpha_2^3(2\eta(\alpha_1^3-\alpha_2^3)+\alpha_2^3)}{D_{EB}^h} \tag{82}$$

$$d_{2h} = \frac{((\alpha_1^3-\alpha_2^3)(4\eta^2-4\eta)-\alpha_2^3)\alpha_1^3\alpha_2^3}{D_{EB}^h} \tag{83}$$

$$d_{3h} = \frac{((\alpha_1^3-\alpha_2^3)(8\eta^3-12\eta^2+6\eta)+\alpha_2^3)\alpha_1^3\alpha_2^3}{D_{EB}^h} \tag{84}$$

and

$$D_{EB}^h = 16((\eta-1/2)^4\,{\alpha_2}^6 - 2\,\eta\,{\alpha_1}^3\,(\eta-1/2)\left(\eta^2-\eta/2+1/2\right){\alpha_2}^3 + {\alpha_1}^6\eta^4) \tag{85}$$

Eqs. (74)–(77) and (81) can be directly used to calculate equivalent in-plane elastic properties of general stepped lattices. The expressions are applicable to both the stepped-up and stepped-down lattices shown in Fig. 1. As a special case, when the lattice is uniform, considering the limiting values shown in Eqs. (44)–(48), it is easy to demonstrate that Eqs. (74)–(77) and (81) reduce to the corresponding equations derived in Ref. [50]. Further, ignoring the axial stretching effect (that is $a_1\to\infty$, more on this is available in the Section 5), it can be easily shown that the new general expressions derived here reduce to the classical equivalent expressions by Gibson and Ashby [5] as a further special case.

Eqs. (74)–(77) and (81) derived here considering a hexagonal lattice configuration as depicted in Fig. 1. However, these expressions are general and they can be used for other type of lattices for specific geometric parameters. In the Section 5, exact closed-form expressions of the equivalent elastic properties are derived for stepped auxetic hexagonal lattices ($\theta = -\theta$), stepped rhombus lattices ($\beta = 0$) and stepped rectangular lattices ($\theta = 0$).

3.4.2. Equivalent elastic moduli with Timoshenko beam theory

In this section, the closed-form expressions for stepped lattice are obtained considering thick beam assumptions for the constituent beam members. The shear deformation effects are significant for beams with a length-to-depth ratio of less than 5. Timoshenko beam theory, which considers the shear contribution [54], is more suitable for such beams. Considering the stiffness coefficients form Eq. (56), the generalised expressions for the equivalent elastic properties for the mass conserved hexagonal stepped lattice are derived in closed-form as

$$E_1 = \frac{\bar{d}_1 E\alpha^3 \cos\theta}{(\beta+\sin\theta)\left(\sin^2\theta + \alpha^2\frac{\bar{d}_1}{a_1}\cos^2\theta\right)} \tag{86}$$

$$E_2 = \frac{\bar{d}_1 E\alpha^3(\beta+\sin\theta)}{\cos^3\theta\left(1+\alpha^2\frac{\bar{d}_1}{a_1}\tan^2\theta + 2\alpha^2\beta\frac{\bar{d}_1}{a_1}\sec^2\theta\right)} \tag{87}$$

$$\nu_{12} = \frac{\left(1-\alpha^2\frac{\bar{d}_1}{a_1}\right)\sin\theta\cos^2\theta}{(\beta+\sin\theta)\left(\sin^2\theta+\alpha^2\frac{\bar{d}_1}{a_1}\cos^2\theta\right)} \tag{88}$$

$$\text{and}\quad \nu_{21} = \frac{(1-\alpha^2\frac{\bar{d}_1}{a_1})\sin\theta(\beta+\sin\theta)}{\left(1+\alpha^2\frac{\bar{d}_1}{a_1}\tan^2\theta+2\alpha^2\beta\frac{\bar{d}_1}{a_1}\sec^2\theta\right)\cos^2\theta} \tag{89}$$

The generalised expression of the shear modulus (Eq. (12)) consists of five stiffness coefficients from the two constituent beam members. There are the two coefficients, $K_{65} = -6EI\bar{d}_2/L^2$ and $K_{44} = EAa_1/L$ from the inclined members and three coefficients from the verticle member. The coefficients from the vertical member are given by

$$K_{55}^{h/2} = \frac{12EI}{(h/2)^3}d_{1h} \tag{90}$$

$$K_{56}^{h/2} = -\frac{6EI}{(h/2)^2}d_{2h} \tag{91}$$

$$\text{and}\quad K_{66}^{h/2} = \frac{4EI}{(h/2)}d_{3h} \tag{92}$$

The closed-form equation for the shear modulus is then obtained by substituting the expressions of the stiffness coefficients in Eq. (12), resulting

$$G_{12} = \frac{E\alpha^3\cos\theta(\beta+\sin\theta)a_1d_2\left(4d_{1h}d_{3h}-3d_{2h}^2\right)}{\left(2a_1d_2\beta+\left(a_1-\alpha^2d_2\right)\left(4d_{1h}d_{3h}-3d_{2h}^2\right)\right)\beta^2\cos^2\theta + d_2\alpha^2\left(1+2\beta\sin\theta+\beta^2\right)\left(4d_{1h}d_{3h}-3d_{2h}^2\right)} \tag{93}$$

In the above

$$d_{1h} = \frac{\alpha_1^3\alpha_2^3(2\eta(\alpha_1^3-\alpha_2^3)+\alpha_2^3)}{D_{TB}^h} \tag{94}$$

$$d_{2h} = \frac{((\alpha_1^3-\alpha_2^3)(4\eta^2-4\eta)-\alpha_2^3)\alpha_1^3\alpha_2^3}{D_{TB}^h} \tag{95}$$

$$d_{3h} = \frac{(((\alpha_1^3-\alpha_2^3)(8\eta^3-12\eta^2+6\eta)+\alpha_2^3)+\Phi\alpha_1^2\alpha_2^2(2\eta(\alpha_1-\alpha_2)+\alpha_2))\alpha_1^3\alpha_2^3}{D_{TB}^h} \tag{96}$$

and

$$D_{TB}^h = 4\left(\left(\Phi{\alpha_1}^2+4\eta^2-4\eta+1\right)(\eta-1/2)^2{\alpha_2}^6-\eta(\eta-1/2)\Phi{\alpha_1}^3{\alpha_2}^5 - \eta\left(\Phi{\alpha_1}^2+8\eta^2-4\eta+4\right)(\eta-1/2){\alpha_1}^3{\alpha_2}^3 + \Phi{\alpha_1}^6{\alpha_2}^2\eta^2+4{\alpha_1}^6\eta^4\right) \tag{97}$$

Eqs. (86)–(89) and (93) can be directly used to calculate equivalent in-plane elastic properties of general stepped lattices. The expressions are applicable to both the stepped-up and stepped-down lattices shown in Fig. 1. As a special case, when the lattice is uniform, considering the limiting values shown in Eqs. (63)–(67), it is easy to demonstrate that Eqs. (86)–(89) and (93) reduce to the corresponding equations derived in Ref. [50]. Again, the expressions for regular case reduce to closed form expressions corresponding to the Euler–Bernoulli case in for $\Phi = 0$. Further, ignoring the axial stretching effect (that is, $a_1 \to \infty$), it can be easily shown that the new general expressions derived here reduce to the classical equivalent expressions by Gibson and Ashby [5] as a further special case.

Eqs. (86)–(89) and (93) are derived considering the hexagonal lattice configuration as in Fig. 1. However, these expressions are general and they can be used for other type of lattices for specific geometric parameters. Following the procedure in the Section 5, exact closed-form expressions of the equivalent elastic properties can be derived for stepped auxetic hexagonal lattices ($\theta = -\theta$), stepped rhombus lattices ($\beta = 0$) and stepped rectangular lattice ($\theta = 0$) with Timoshenko beam theory.

4. Numerical results and discussions

Numerical results obtained for the stepped lattice are investigated in detail. The distribution of the material of the constituent beam member is considered in such a way that it maintains the same mass as the regular lattice. Considering the redistribution of the mass, some insightful results are obtained which are described in the following subsections.

4.1. Comparison between the two proposed approaches

We explore the possibility of different values of the equivalent elastic properties of stepped lattices obtained using two different approaches developed in the paper. These approaches are (1) the static condensation based method prosed in Section 3.2, and (2) the Castigliano's method based formulation in Section 3.3. Fig. 6 represents the comparison between two approaches considering the normalised values of E_1 and ν_{12}. Eqs. (74) and (76) are utilised to obtain the analytical curves for E_1 and ν_{12}, respectively. They show that the results are close to each other. Through the static condensation-based approach, one can exploit the power of the finite element method for complex geometries. For such cases, the analytical Castigliano based approach may result in longer expressions in the closed-form equations. On the other hand, the Castigliano based approach is straightforward for most of the geometries, and a closed-form solution can be obtained. It can also be observed that by varying the value of α_2, a huge range of values for Young's modulus can be obtained while keeping the overall mass of the lattice almost the same. This is a significant advantage compared to the classical regular lattice.

4.2. Comparison between Euler–Bernoulli and Timoshenko beam theory

The equivalent elastic properties obtained considering both Euler–Bernoulli beam theory and Timoshenko beam theory are compared. The closed-form expressions to perform the comparative study were derived in Sections 3.4.1 and 3.4.2. We can observe from Fig. 7 that there are minor differences in the values when different theories are considered. It is noticed that the Euler–Bernoulli assumption shows a slightly higher value for the value of equivalent Young's modulus. This is expected because it neglects the shear contribution in the deformation, which results in a smaller value of displacements followed by a higher E_1 value. It is observed that for higher values of α_2, the

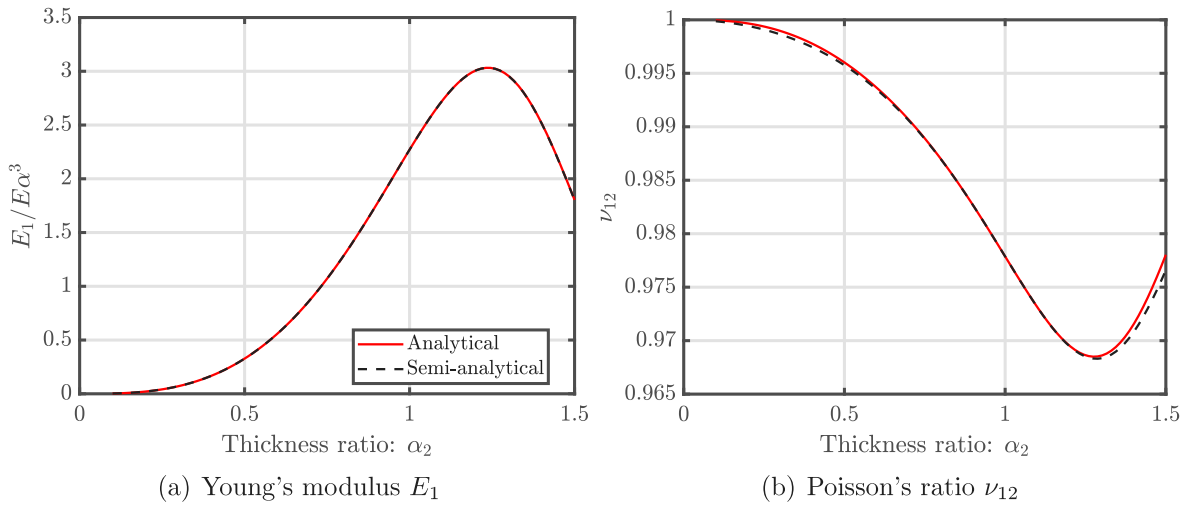

(a) Young's modulus E_1 (b) Poisson's ratio ν_{12}

Fig. 6. Comparison between analytical (Castigliano based approach) and semi analytical (static condensation) results for stepped lattice considering Euler–Bernoulli beam theory for the constituent beam member. Numerical values used are: the stepping length ratio $\eta = 0.25$, the cell angle $\theta = 30°$ and the height ratio $\beta = h/L = 1$.

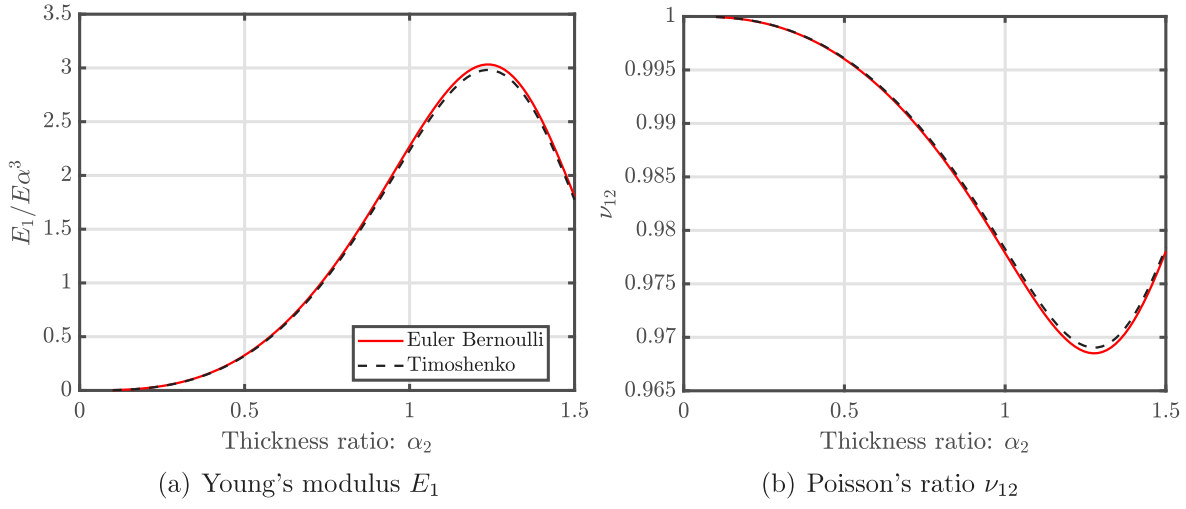

(a) Young's modulus E_1 (b) Poisson's ratio ν_{12}

Fig. 7. Comparison of results for stepped lattices considering Euler–Bernoulli and Timoshenko beam theory for constituent beam members considering the stepping length ratio $\eta = 0.25$, the cell angle $\theta = 30°$ and the height ratio $\beta = h/L = 1$.

difference between the two approaches are more. This is because higher values of α_2 represent a thicker beam at a certain part of the section and consequently higher impact of the shear deformation. Based on this analysis, it is recommended that analytical expressions based on Timoshenko beam theory given in Section 3.4.2 should be used when $\alpha_2 > 1$.

4.3. Effect of geometric parameters on the equivalent elastic properties

A novel aspect of the stepped lattices compared to a regular lattice is the impact of the different geometric parameters on the equivalent material properties of the lattice. The physical nature of the plots considering Euler–Bernoulli and Timoshenko beam theory is similar. Therefore, results using the case of Euler–Bernoulli theory is shown. Fig. 8 shows the normalised equivalent elastic moduli and Poisson's ratios obtained for the regular stepped hexagonal lattice considering different α_2 values and $\eta = 0.30$. The values of the stepping height ratio determine if the lattice is stepped-up or stepped-down. The stepped-down lattice is identified by $\alpha_2 > 1$ and $\alpha_2 < 1$ denotes a stepped-up lattice. The curves of $\alpha_2 = 1$, which corresponds to the regular lattice, lie between other cases. It is evident from the plots that the stepping height ratio has a significant effect on the equivalent elastic properties of the lattice with different cell angles, and various values can be obtained depending upon the design requirements. Also, it is evident from the results that higher values for the elastic properties cannot be obtained by simply increasing the α_2 values. There should be a particular value for that the elastic properties could be the maximum.

Fig. 9 shows the effect of stepping length ratio (η) on the elastic properties keeping $\alpha_2 = 1.30$. It is observed that the effect of η is not that significant for lattices with different cell angles. To visualise of the effect of different α_2 values on the lattice with different θ values a 3D plot Fig. 10 is obtained. From the plot, it is evident that for a particular α_2 value, we are getting maximum values of Young's modulus for every cell angle. The α_2 has much influence on every elastic property. Whereas, Fig. 11 shows that η has similar kinds of effects for each elastic property. Also, for $\eta = 0.30$, the values of Young's modulus are reaching maximum values for all cell angles. The effect of the geometric parameters α_2 and η are also explored for G_{12} and Fig. 12 shows that. Figure Fig. 12(a) shows the normalised G_{12} as a function of cell angle θ for $\eta = 0.3$ considering various α_2 values. Figure Fig. 12(b) shows normalised G_{12} as a function of cell angle θ for $\alpha_2 = 1.3$ considering various η values. The plots show that the nature of the curves are different from the same plots of E_1. The value of G_{12} is getting higher for lower η values unlike E_1. From Fig. 12(a)

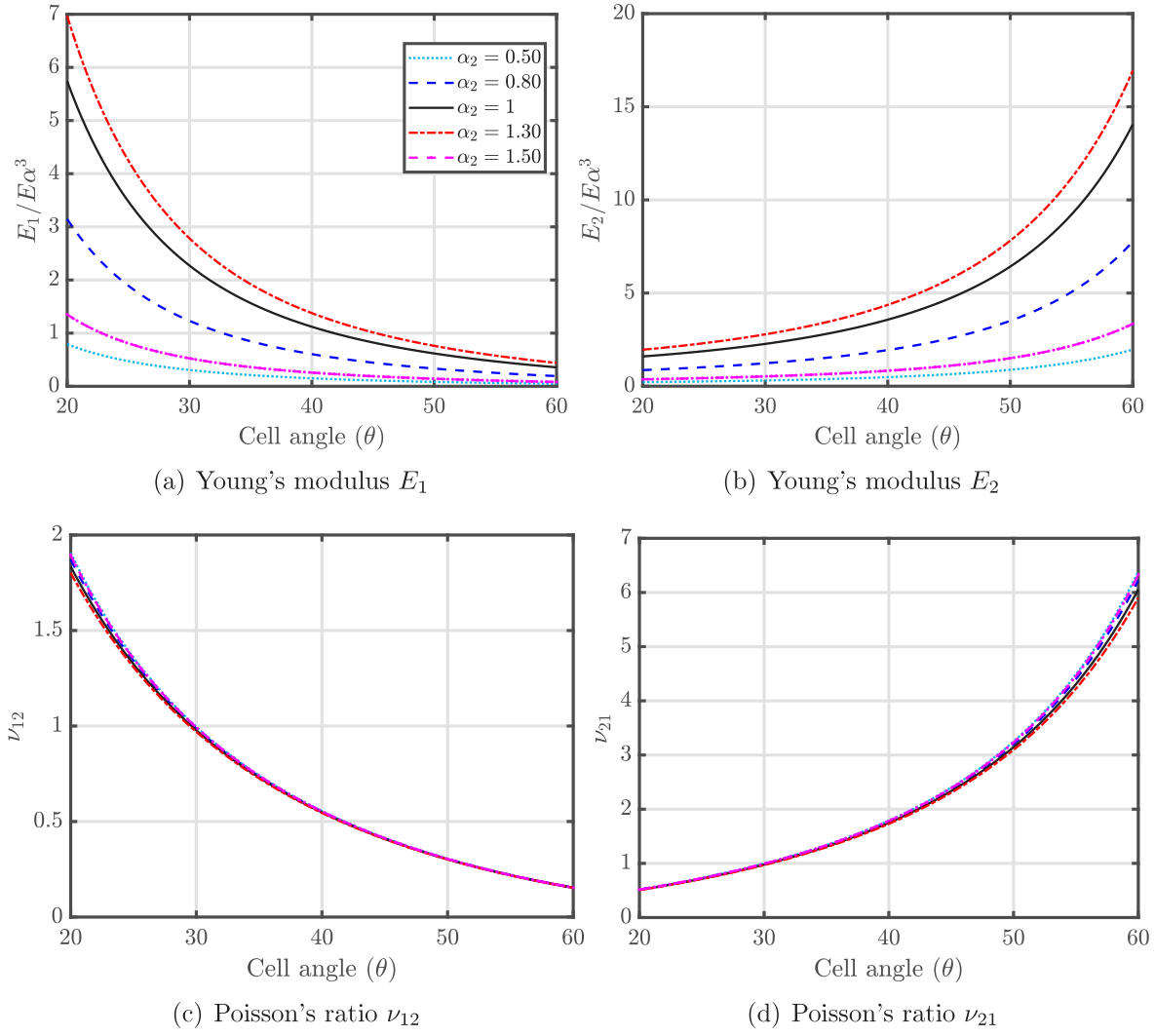

Fig. 8. Normalised equivalent elastic moduli and Poisson's ratio obtained for stepped hexagonal lattice as a function of cell angle (θ) considering various stepping height ratio (α_2) values. The height ratio is $\beta = h/L = 1$ and the stepping length ratio is $\eta = 0.30$.

it is not quite clear for what values of α_2 the value of G_{12} is reaching towards maximum as we only obtained that plot for a particular $\eta = 0.3$. To get the clear picture 3D plots are obtained (see figures Fig. 12(c) and (d)). The 3D plot for G_{12} as a function of α_2 and θ is similar to E_1 but not exactly the same. One can notice that here also for a particular value of α_2 the G_{12} is obtaining maximum value for all θ values. The region of α_2 for which G_{12} is geting maximum is also close to the same as E_1. Whereas, The plot of G_{12} as a function of η and θ is qite different from the same plot of E_1 and here its the reverse. The G_{12} is obtaining higher values for η values in the lower region for all θ. To investigate the effect of the redistribution of mass of the constituent beam members keeping the total mass almost the same for the whole lattice, a 3D plot Fig. 13 is obtained as a function of η and α_2. It is noticed that by redistributing the mass of the beam user-defined material properties can be achieved for the lattice. The trend for the E_1 and E_2 are the same. Whereas, the nature of G_{12} is a bit different. At first the normalised values of E_1 and ν_{12} are shown followed by the plot of G_{12} (see Fig. 14). The normalisation is performed dividing E_1, ν_{12} and G_{12} obtained from Eqs. (74), (76) and (81) respectively by their corresponding values considering a regular lattice with prismatic beam as constituent members. The equivalent elastic properties for the regular lattice are termed as E_1^{reg}, ν_{12}^{reg} and G_{12}^{reg}. The closed-form expressions for the equivalent regular lattice are obtained considering the Eqs. (8) and (10) as

$$E_1^{\text{reg}} = \frac{E\alpha^3 \cos\theta}{(\beta + \sin\theta)\left(\sin^2\theta + \alpha^2\cos^2\theta\right)} \tag{98}$$

$$\nu_{12}^{\text{reg}} = \frac{\left(1-\alpha^2\right)\sin\theta\cos^2\theta}{(\beta + \sin\theta)\left(\sin^2\theta + \alpha^2\cos^2\theta\right)} \tag{99}$$

$$\text{and} \quad G_{12}^{\text{reg}} = \frac{E\alpha^3(\beta + \sin\theta)}{(\beta^2(1+2\beta) + \alpha^2(\cos\theta + (\beta + \sin\theta)\tan\theta)^2)\cos\theta} \tag{100}$$

The characteristics of Poisson's ratios are also the same. The trend of the plots shows that for a particular value of η and α_2, the elastic properties can obtain maximum values. Also, the range of the values is quite large, which are obtained by redistributing the mass of the constituent beam member of a regular hexagonal lattice. In this research, the effect of the joints is neglected. This means the masses of the lattices for different η and α_2 values may not be the same but quite close. Results show a larger design space of the stepped lattice in comparison to the conventional regular hexagonal lattice.

Fig. 15(a) and (b) shows the normalised E_1 and G_{12} for a lattice with cell angle 30° as a function of stepping height ratio α_2 for different η values. It shows that for a particular α_2 value, the material property is going to have maximum value for each η. A very low value of η and α_2 will inhibit the manufacturing constraint. So, the range of η and α_2 are fixed according to manufacturing feasibility. The feasible region of the

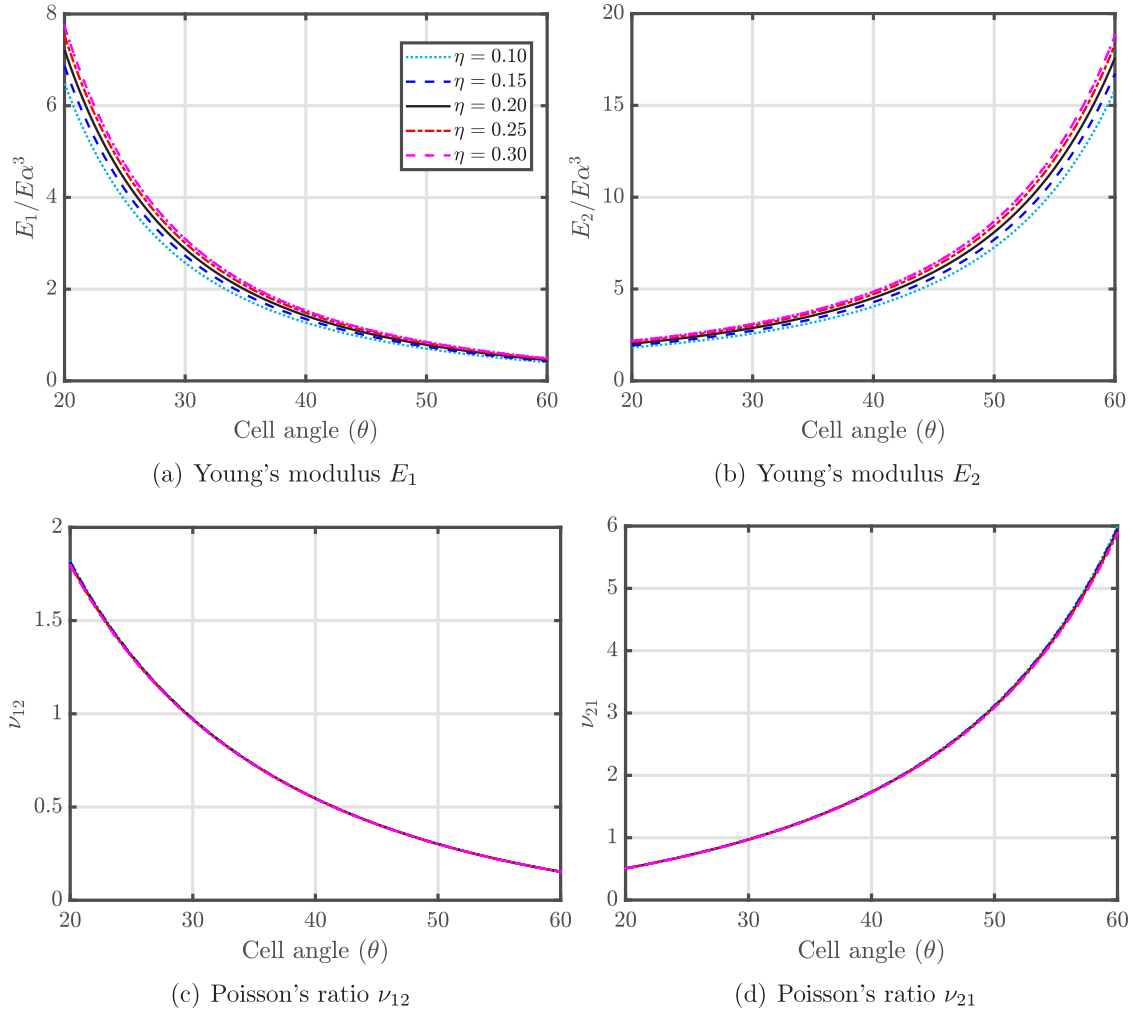

Fig. 9. Normalised equivalent elastic moduli and Poisson's ratio obtained for stepped hexagonal lattice as a function of cell angle (θ) considering various stepping length ratio (η) values. The height ratio is $\beta = h/L = 1$ and the stepping height ratio is $\alpha_2 = 1.30$.

geometric parameters has already been discussed in Section 2.2. The value of the material property increases with α_2 at the beginning, but it is not monotonic. It decreases after certain values of α_2. The nature of the curve also depends upon the η value. This study shows that there should be a particular value of η and α_2 for that maximum value can be reached. It is also observed that for lower η values the sensitivity of both E_1 and G_{12} decreases with α_2. The curves become more flat with decreasing η values. The difference between the characteristics of E_1 and G_{12} is that for larger η values the E_1 is approaching towards maxima whereas, for G_{12} it is the reverse. Let us consider the curve corresponding to $\eta = 0.3$ from 15(a) and (c). It can be observed that while the value of E_1 is reaching to its maximum near $\alpha_2 = 1.2$ the value of G_{12} obtain about 30% lesser value from the regular lattice. It is also noticed that in some cases, there are two design values of α_2, which give the same elastic modulus. This implies that two very different geometric designs can give the same equivalent elastic moduli. This is a special feature of stepped lattices, which is very different from regular lattices. Fig. 15(b) and (d) show the variation of normalised E_1 and G_{12} respectively, with η for different values of α_2. It show that for $\alpha_2 = 1$ there is no variation for the values of E_1 and G_{12} with η. For G_{12}, the nature of the curves corresponding to $\alpha_2 = 1.2$ and 1.3 are different from the same plot of E_1. In both cases (E_1 and G_{12}) the maxima seems to occur for α_2 close to 1.2. One can observe that for $\alpha_2 = 1.2$ and 1.3 we are getting almost 20% and 30% higher value of E_1 than the regular case, respectively. While the value of G_{12} is getting lower by 60% and 25% for the corresponding vlues of α_2. This indicates that a structure with low shear moduls can be formed by redistributing the mass while maximising the Young's modulus (2D pentamode type of structures). It can be observed that the possibilities are huge to obtain large variation in the equivalent material properties. The values can be a very low value to a very high one. The additional parameters, α_2 and η along with θ can be utilised to tune the equivalent properties as per the user-defined design.

5. Special cases of the general expressions

The analytical expressions of the equivalent elastic properties for the stepped hexagonal are derived in Section 3. The generalised expressions from the Euler–Bernoulli case mentioned in Section 3.4.1 are utilised. The respective Eqs. are (74), (75), (76), (77) and (81). The generalised formulation is applied to various other lattice patterns and geometry of the constituent members. The closed-form expressions of the equivalent elastic properties for four special cases are obtained by limiting the geometric parameters. Geometries of three specific lattices are shown in Fig. 16. They include: the stepped auxetic hexagonal lattice ($\theta = -\theta$), the stepped rhombus lattice ($\beta = 0$) and the stepped rectangular lattice ($\theta = 0$). The lattices shown in Fig. 16 are stepped-up lattices. Equivalent stepped-down lattices can be obtained following similar geometric designs. The closed-form expressions derived below are for mass-conserved lattices, valid for both stepped-up and stepped-down cases.

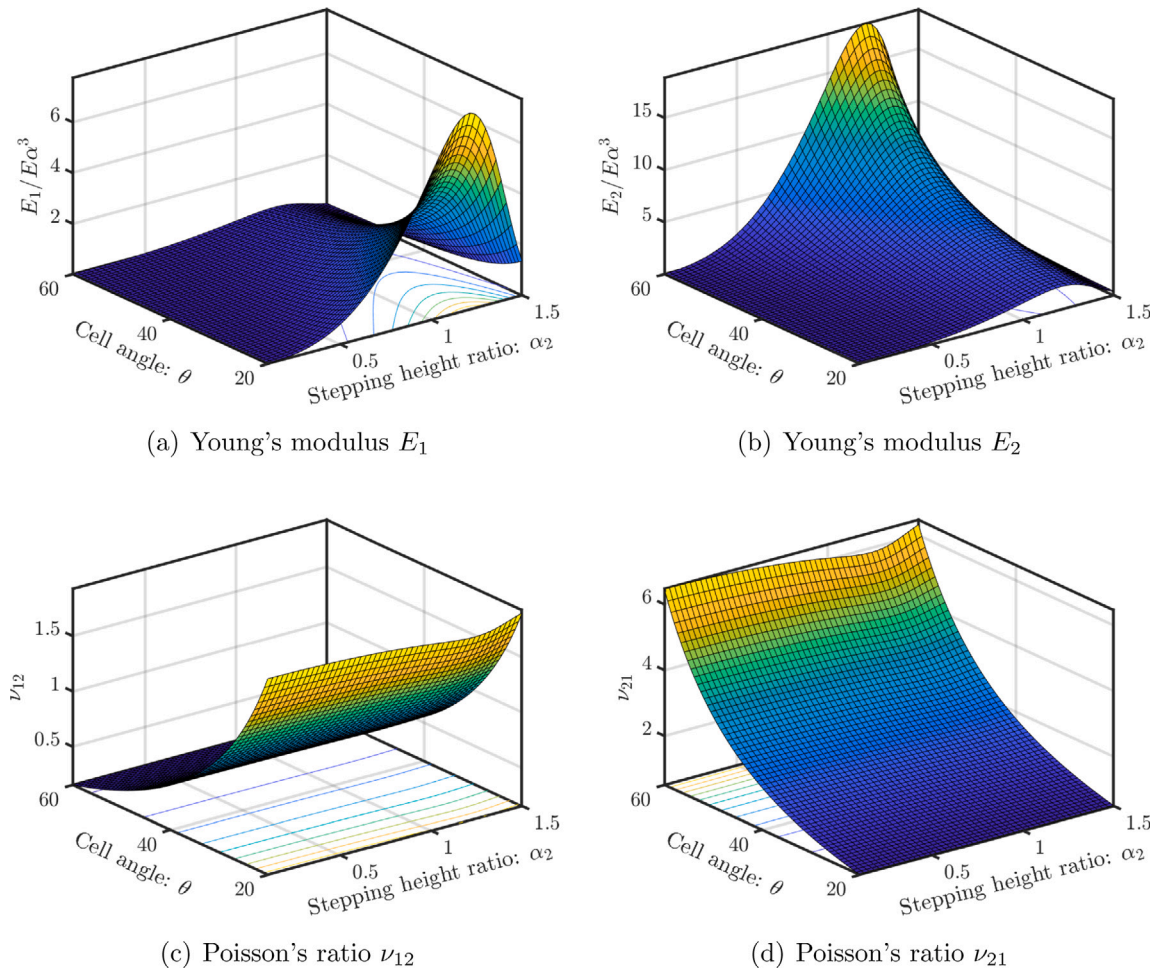

Fig. 10. Normalised equivalent elastic moduli and Poisson's ratio obtained for hexagonal mass conserved stepped lattice. The results are plotted as functions of stepping height ratio (α_2) and cell angle (θ) for a value of height ratio $\beta = h/L = 1$ and $\eta = 0.30$.

5.1. Axially rigid stepped lattices

The closed-form expressions of axially rigid stepped lattice are obtained considering $a_1 \to \infty$. Imposing this limiting case, from Eqs. (74)–(77) and (81) one obtains

$$E_1 = E\alpha^3 \frac{\cos\theta}{(\beta + \sin\theta)\sin^2\theta} d_1 \tag{101}$$

$$E_2 = E\alpha^3 \frac{(\beta + \sin\theta)}{\cos^3\theta} d_1 \tag{102}$$

$$\nu_{12} = \frac{\cos^2\theta}{(\beta + \sin\theta)\sin\theta} \tag{103}$$

$$\nu_{21} = \frac{(\beta + \sin\theta)\sin\theta}{\cos^2\theta} \tag{104}$$

and

$$G_{12} = \frac{E\alpha^3(\beta + \sin\theta)}{\beta^2\cos\theta} \frac{d_2\left(4\,d_{1h}\,d_{3h} - 3\,{d_{2h}}^2\right)}{\left(2\,\beta\,d_2 + 4\,d_{1h}\,d_{3h} - 3\,{d_{2h}}^2\right)} \tag{105}$$

Numerical results show that these simple formulae give acceptable accuracy for $\alpha \leq 0.2$. These expressions match with the classical Gibson and Ashby [5] formulas for a regular hexagonal lattice ($d_1 = 1, d_2 = 1$). This illustrates the general nature of the analytical expressions derived in this present study.

5.2. Auxetic stepped lattices: $\theta < 0$

The closed-form expressions for the equivalent elastic properties of stepped re-entrant lattice (Fig. 16(a)) are obtained by considering $\theta = -\theta$ to the expressions derived in Section 3.4.1. The closed-form expressions of auxetic stepped hexagonal lattice are

$$E_1 = \frac{d_1 E\alpha^3 \cos\theta}{(\beta - \sin\theta)\left(\sin^2\theta + \alpha^2 \frac{d_1}{a_1}\cos^2\theta\right)} \tag{106}$$

$$E_2 = \frac{d_1 E\alpha^3(\beta - \sin\theta)}{\cos^3\theta\left(1 + \alpha^2\frac{d_1}{a_1}\tan^2\theta + 2\alpha^2\beta\frac{d_1}{a_1}\sec^2\theta\right)} \tag{107}$$

$$\nu_{12} = -\frac{\left(1 - \alpha^2\frac{d_1}{a_1}\right)\sin\theta\cos^2\theta}{(\beta - \sin\theta)\left(\sin^2\theta + \alpha^2\frac{d_1}{a_1}\cos^2\theta\right)} \tag{108}$$

$$\nu_{21} = -\frac{\left(1 - \alpha^2\frac{d_1}{a_1}\right)\sin\theta(\beta - \sin\theta)}{\left(1 + \alpha^2\frac{d_1}{a_1}\tan^2\theta + 2\alpha^2\beta\frac{d_1}{a_1}\sec^2\theta\right)} \tag{109}$$

and

$$G_{12} = \frac{E\alpha^3\cos\theta(\beta - \sin\theta)a_1 d_2\left(4d_{1h}d_{3h} - 3{d_{2h}}^2\right)}{\left(2a_1d_2\beta + \left(a_1 - \alpha^2 d_2\right)\left(4d_{1h}d_{3h} - 3{d_{2h}}^2\right)\right)\beta^2\cos^2\theta + d_2\alpha^2\left(1 - 2\beta\sin\theta + \beta^2\right)\left(4d_{1h}d_{3h} - 3{d_{2h}}^2\right)} \tag{110}$$

The expressions for the regular hexagonal auxetic lattice can be obtained considering the limiting case when $d_1 = a_1 = 1$.

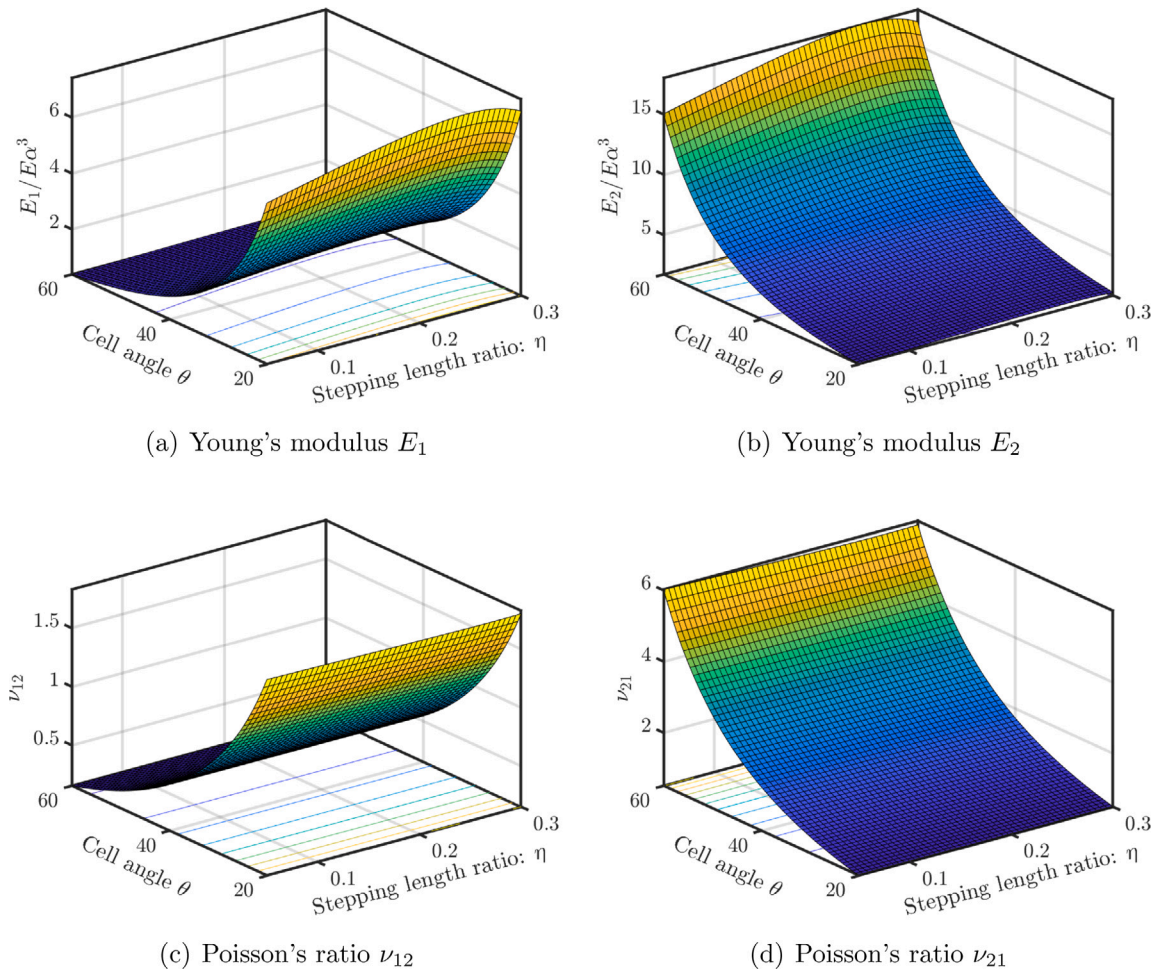

Fig. 11. Normalised equivalent elastic moduli and Poisson's ratio obtained for hexagonal mass conserved stepped lattice. The results are plotted as functions of stepping length ratio (η) and cell angle (θ) for a value of height ratio $\beta = h/L = 1$ and $\alpha_2 = 1.30$.

5.3. Rombus stepped lattices: $\beta = 0$

The rhombus stepped lattice, shown in Fig. 16(b) is obtained by removing the vertical member from the unit cell. Mathematically the expressions of the equivalent elastic properties for the regular rhombus lattice are obtained considering $\lim_{\beta\to 0}$ to the expressions derived in Section 3.4.1. The closed-form expressions are given by

$$E_1 = \frac{d_1 E\alpha^3 \cos\theta}{\sin\theta\left(\sin^2\theta + \alpha^2 \frac{d_1}{a_1}\cos^2\theta\right)} \tag{111}$$

$$E_2 = \frac{d_1 E\alpha^3 (\sin\theta)}{\cos^3\theta\left(1 + \alpha^2 \frac{d_1}{a_1}\tan^2\theta + 2\alpha^2\beta\frac{d_1}{a_1}\sec^2\theta\right)} \tag{112}$$

$$\nu_{12} = \frac{\left(1 - \alpha^2\frac{d_1}{a_1}\right)\cos^2\theta}{\sin^2\theta + \alpha^2\frac{d_1}{a_1}\cos^2\theta} \tag{113}$$

$$\nu_{21} = \frac{\left(1 - \alpha^2\frac{d_1}{a_1}\right)\sin^2\theta}{1 + \alpha^2\frac{d_1}{a_1}\tan^2\theta + 2\alpha^2\beta\frac{d_1}{a_1}\sec^2\theta} \tag{114}$$

and

$$G_{12} = E\alpha a_1 \sin\theta\cos\theta \tag{115}$$

The expressions for the regular rhombus lattice can be obtained by substituting $d_1 = a_1 = 1$.

5.4. Rectangular stepped lattices: $\theta = 0$

The stepped rectangular lattice is formed when $\theta = 0$ and is shown in Fig. 16(c). The expressions of the equivalent elastic properties for the stepped rectangular lattice are obtained by considering $\lim_{\theta\to 0}$ to the expressions derived in Section 3.4.1. After some simplifications, one obtains

$$E_1 = \frac{E\alpha}{\beta}a_1 \tag{116}$$

$$E_2 = \frac{E\alpha^3\beta}{1 + 2\alpha^2\beta\frac{d_1}{a_1}}d_1 \tag{117}$$

$$\nu_{12} = 0, \quad \nu_{21} = 0 \tag{118}$$

and

$$G_{12} = \frac{E\alpha^3(\beta)\, a_1 d_2\left(4d_{1h}d_{3h} - 3{d_{2h}}^2\right)}{\left(2a_1 d_2\beta + \left(a_1 - \alpha^2 d_2\right)\left(4d_{1h}d_{3h} - 3{d_{2h}}^2\right)\right)\beta^2 + d_2\alpha^2\left(1+\beta^2\right)\left(4d_{1h}d_{3h} - 3{d_{2h}}^2\right)} \tag{119}$$

The expressions for the regular rectangular lattice are obtained when $d_1 = a_1 = 1$.

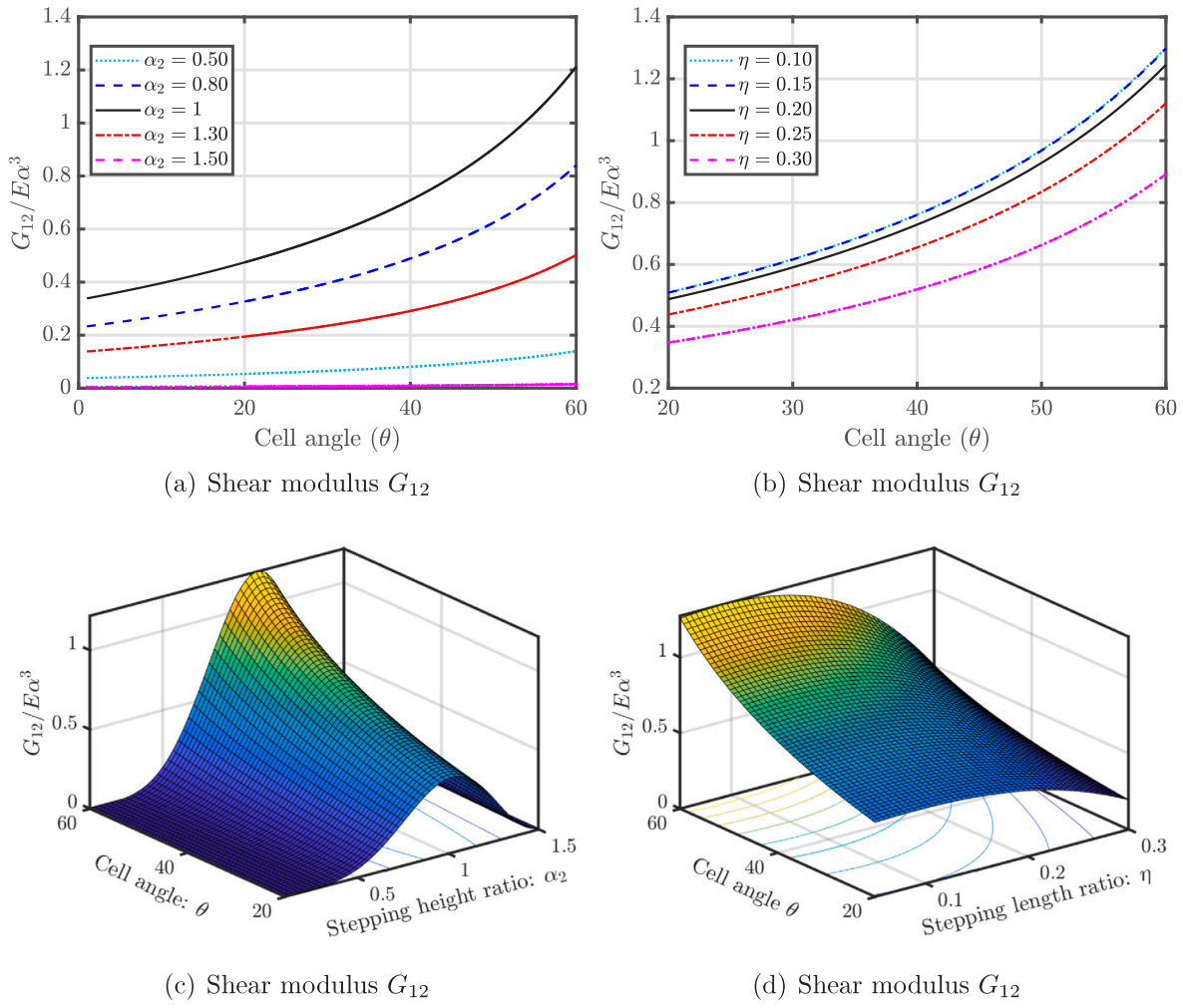

(a) Shear modulus G_{12} (b) Shear modulus G_{12}

(c) Shear modulus G_{12} (d) Shear modulus G_{12}

Fig. 12. Normalised equivalent shear modulus obtained for stepped hexagonal lattice as a function of (a) cell angle (θ) considering various stepping height ratio (α_2) values keeping $\eta = 0.30$, (b) cell angle (θ) considering various stepping length ratio (η) values keeping $\alpha_2 = 1.30$, (c) cell angle (θ) and stepping height ratio (α_2) and (d) cell angle (θ) and stepping length ratio (η). The height ratio is $\beta = h/L = 1$.

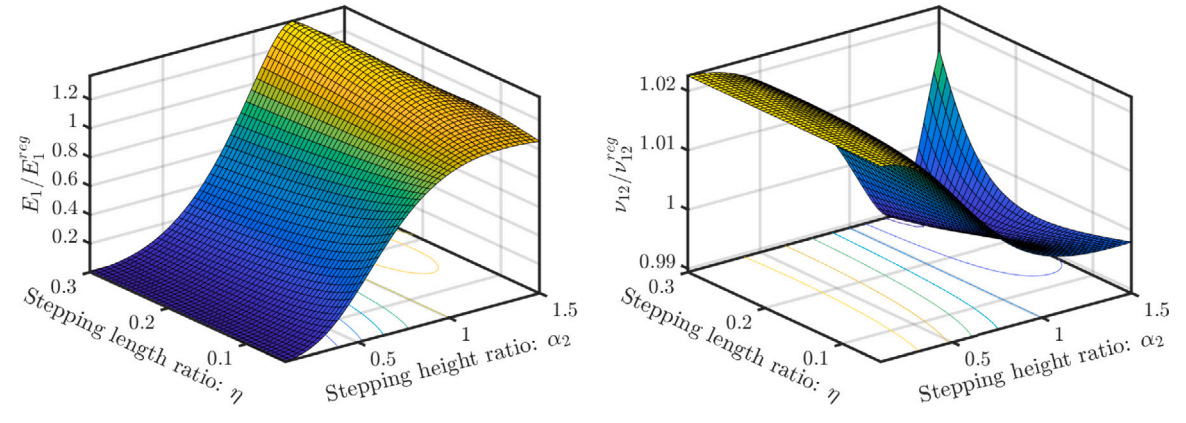

(a) Young's modulus E_1 (b) Poisson's ratio ν_{12}

Fig. 13. Normalised equivalent elastic modulus and Poisson's ratio obtained for hexagonal mass conserved stepped lattice. The results are plotted as functions of stepping length ratio η and stepping height ratio α_2 for a value of height ratio $\beta = h/L = 1$. The value of cell angle $\theta = 30°$.

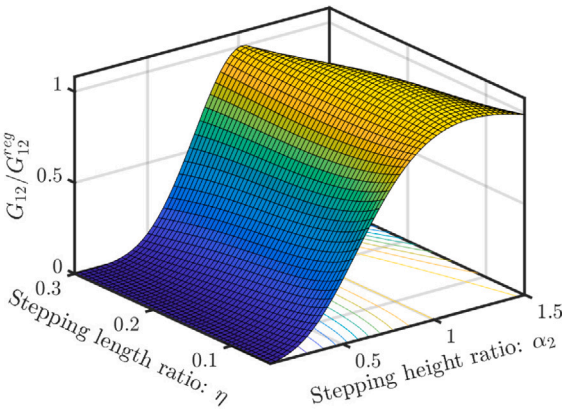

Fig. 14. Normalised equivalent shear modulus (G_{12}) obtained for hexagonal mass conserved stepped lattice. The results are plotted as functions of stepping length ratio η and stepping height ratio α_2 for a value of height ratio $\beta = h/L = 1$. The value of cell angle $\theta = 30°$.

A similar approach can also be followed to obtain the closed-form expressions for the different cases considering the Timoshenko beam theory mentioned in Section 3.4.2.

6. Optimal lattice geometry

In this section, the optimum values of the geometric parameters are obtained followed by the normalised maximum value of the material parameter E_1. To obtain the values of the geometric parameters the Eq. (120) is used. The contributions from the axial part are excluded for simplifications (see Section 5.1 for the relevant expressions). The closed-form expression of E_1 becomes

$$E_1 = \underbrace{\frac{E\alpha^3\cos\theta}{(\beta+\sin\theta)\sin^2\theta}}_{E_1^{GA}} d_1 \tag{120}$$

where E_1^{GA} denotes the equivalent elastic modulus of a regular hexagonal lattice ignoring axial deformation of the constituent beams as given by Gibson and Ashby [5]. The Eq. (40) shows that d_1 is a function of η and α_2 so as E_1. For a regular hexagonal lattice, $d_1 = 1$. Therefore, any value of d_1 more than 1 represents an increase in the stiffness of the stepped lattice compared to a regular lattice. To obtain the maximum value of E_1 analytically we consider the following procedure. The critical points are obtained by solving the following two simultaneous equations

$$\frac{\partial E_1}{\partial \alpha_2} = 0 \tag{121}$$

$$\text{and} \quad \frac{\partial E_1}{\partial \eta} = 0 \tag{122}$$

The optimum values of the geometric parameters can be obtained by checking the sign of the determinant of the Hessian matrix for the critical points. The expression for the Hessian matrix is given by

$$\mathbf{H} = \begin{bmatrix} \frac{\partial^2 E_1}{\partial \alpha_2^2} & \frac{\partial^2 E_1}{\partial \eta \partial \alpha_2} \\ \frac{\partial^2 E_1}{\partial \alpha_2 \partial \eta} & \frac{\partial^2 E_1}{\partial \eta^2} \end{bmatrix} \tag{123}$$

The set of critical points for which the determinant of the Hessian matrix (mentioned in Eq. (123)) is < 0 ensures the criteria for the maximum [55]. The set of two simultaneous equations as a function of the geometric parameters can be obtained by substituting Eq. (120) into Eq.s (121) and (122). Then the simultaneous equations become

$$\frac{\partial E_1}{\partial \alpha_2} = \frac{\partial E_1}{\partial d_1}\frac{\partial d_1}{\partial \alpha_2} = \frac{E\alpha^3\cos\theta}{(\beta+\sin\theta)\sin^2\theta}\frac{\partial}{\partial \alpha_2}\left(\frac{\alpha_1^3\alpha_2^3}{(\alpha_1^3-\alpha_2^3)\left((2\eta-1)^3+1\right)+\alpha_2^3}\right) = 0 \tag{124}$$

$$\text{and} \quad \frac{\partial E_1}{\partial \eta} = \frac{\partial E_1}{\partial d_1}\frac{\partial d_1}{\partial \eta} = \frac{E\alpha^3\cos\theta}{(\beta+\sin\theta)\sin^2\theta}\frac{\partial}{\partial \eta}\left(\frac{\alpha_1^3\alpha_2^3}{(\alpha_1^3-\alpha_2^3)\left((2\eta-1)^3+1\right)+\alpha_2^3}\right) = 0 \tag{125}$$

After performing some algebraic simplifications, the above two equations reduce to two simultaneous nonlinear equations

$$\left(96\eta^5 - 192\eta^4 + 160\eta^3 - 60\eta^2 + 12\eta - 1\right)\alpha_2{}^4 + \left(-128\eta^5 + 192\eta^4 - 96\eta^3\right)\alpha_2{}^3 + \left(96\eta^4 - 144\eta^3 + 72\eta^2\right)\alpha_2{}^2 + \left(-32\eta^3 + 48\eta^2 - 24\eta\right)\alpha_2 + 4\eta^2 - 6\eta + 3 = 0 \tag{126}$$

$$\text{and} \quad \left(16\eta^3 - 4\eta + 1\right)\alpha_2{}^3 + \left(-24\eta^2 + 8\eta - 1\right)\alpha_2{}^2 + (8\eta - 1)\alpha_2 - 1 = 0 \tag{127}$$

These two equations are solved numerically and the optimal parameter values are calculated as

$$(\alpha_2)_{opt} = 1.1972 \tag{128}$$

$$\text{and} \quad (\eta)_{opt} = 0.3195 \tag{129}$$

For these values, d_1 reach a maximum value as

$$(d_1)_{max} = 1.3776 \quad \text{or} \quad (E_1)_{max} = 1.3776\frac{E\alpha^3\cos\theta}{(\beta+\sin\theta)\sin^2\theta} = 1.3776E_1^{GA} \tag{130}$$

In this derivation, the effect of axial deformation is not considered for simplicity. However, applying the same set of optimum values in Eq. (74) the maximum value of E_1 is obtained as $(E_1)_{max}$ as $1.3668E_1^{reg}$. Here E_1^{reg} considers the axial contribution and is defined in Eq. (98). This is very close to what was obtained ignoring the axial contributions. As the optimal value of α_2 is more than one in Eq. (128), the optimal lattice design for a maximum equivalent E_1 is a stepped-down design.

The same approach is followed for obtaining the optimum values of α_2 and η in case of shear modulus G_{12}. The closed-form expression of G_{12} without the axial contribution can be written as

$$\begin{aligned} G_{12} &= \frac{E\alpha^3(\beta+\sin\theta)d_2(4d_{1h}d_{3h} - 3d_{2h}^2)}{\beta^2\cos\theta(2\beta d_2 + (4d_{1h}d_{3h} - 3d_{2h}^2))} \\ &= \frac{E\alpha^3(\beta+\sin\theta)d_2 D_h^2(4d_{1h}d_{3h} - 3d_{2h}^2)}{\beta^2\cos\theta(2\beta d_2 D_h^2 + D_h^2(4d_{1h}d_{3h} - 3d_{2h}^2))} \\ &= \frac{E\alpha^3(\beta+\sin\theta)d_2\bar{N}}{\beta^2\cos\theta(2\beta d_2 D_h^2 + \bar{N})} = \frac{E\alpha^3(\beta+\sin\theta)d_2\bar{N}}{\beta^2\cos\theta\bar{D}} \\ &= \frac{E\alpha^3(\beta+\sin\theta)}{\beta^2\cos\theta}\frac{d_2\bar{N}}{\bar{D}} \end{aligned} \tag{131}$$

Where, $D_h = D_{EB}^h$. d_2 and $\bar{N}$ are functions of α_2 and η. While $\bar{D}$ is function of α_2, η and β.

The critical points are obtained by numerically solving the following two simultaneous equations

$$\frac{\partial G_{12}}{\partial \alpha_2} = \frac{E\alpha^3(\beta+\sin\theta)}{\beta^2\cos\theta}\frac{\bar{D}\frac{\partial}{\partial\alpha_2}(d_2\bar{N}) - (d_2\bar{N})\frac{\partial\bar{D}}{\partial\alpha_2}}{\bar{D}^2} = 0 \tag{132}$$

$$\text{and} \quad \frac{\partial G_{12}}{\partial \eta} = \frac{E\alpha^3(\beta+\sin\theta)}{\beta^2\cos\theta}\frac{\bar{D}\frac{\partial}{\partial\eta}(d_2\bar{N}) - (d_2\bar{N})\frac{\partial\bar{D}}{\partial\eta}}{\bar{D}^2} = 0 \tag{133}$$

The expressions of the two nonlinear equations from (132) and (133) are very lengthy to be produced in the manuscript. The optimal parameter values are calculated for $\beta = 1$ as

$$(\alpha_2)_{opt} = 1.1679 \tag{134}$$

$$\text{and} \quad (\eta)_{opt} = 0.1318 \tag{135}$$

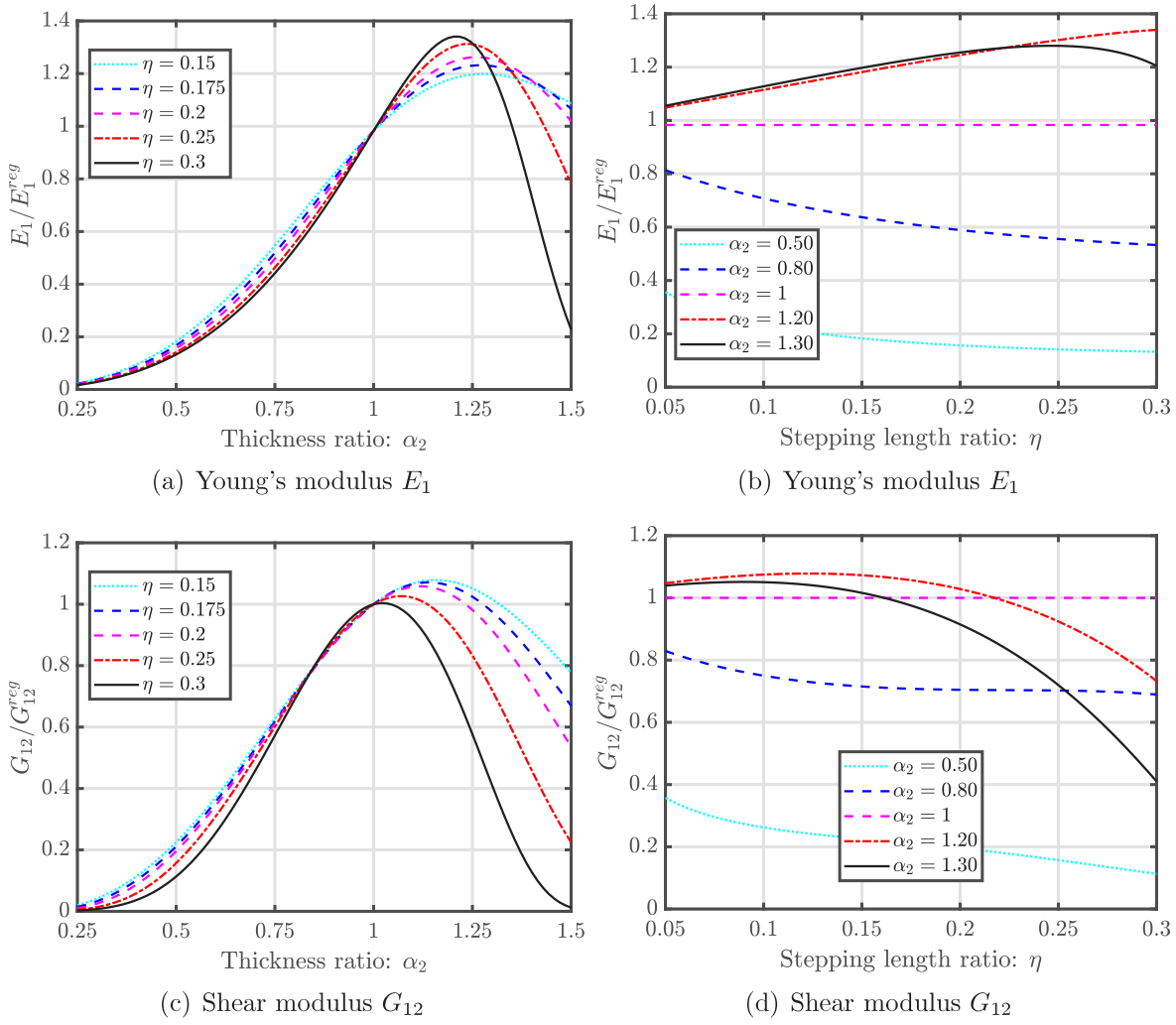

Fig. 15. Normalised (a) E_1 as a function of stepping height ratio (α_2), (b) E_1 as a function of stepping length ratio (η), (c) G_{12} as a function of stepping height ratio (α_2) and (d) G_{12} as a function of stepping length ratio (η) for stepped lattice. The value of cell angle $\theta = 30°$ and the value of height ratio $\beta = h/L = 1$.

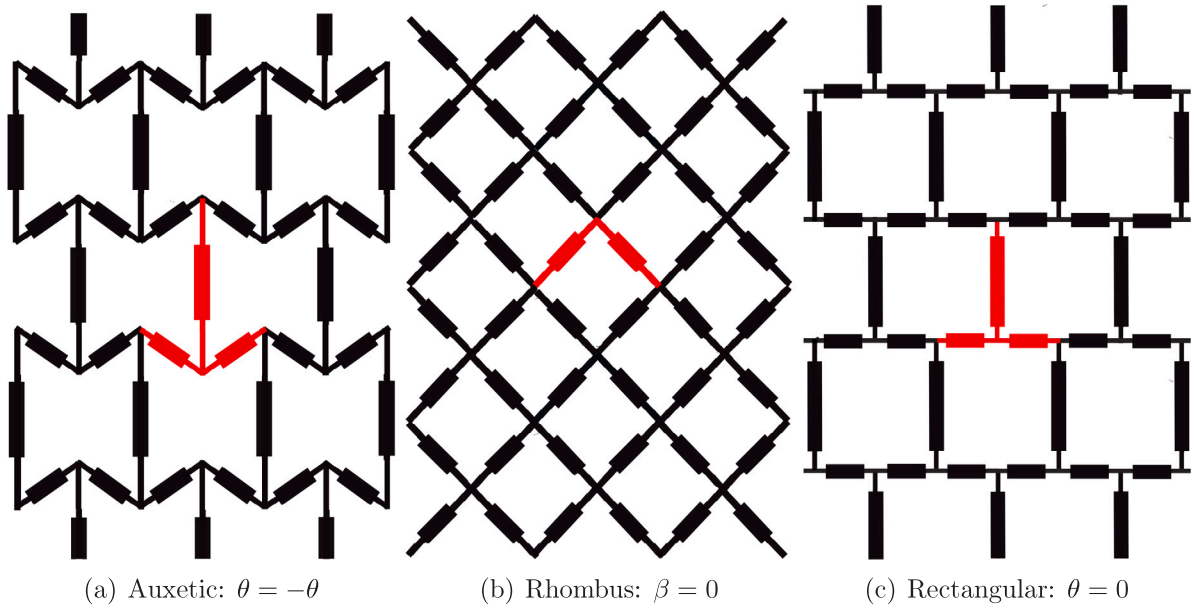

Fig. 16. The geometry of various stepped-up lattices and their corresponding unit cells (equivalent stepped-down lattices can be obtained following similar geometric designs). The family of lattices is created by considering special values of the cell angle (θ) and the height ratio (β). The specific lattices are: (a) the stepped auxetic hexagonal lattice ($\theta = -\theta$), (b) the stepped rhombus lattice ($\beta = 0$) and (c) the stepped rectangular lattice ($\theta = 0$). Unit cells of the stepped lattices are highlighted in the figures.

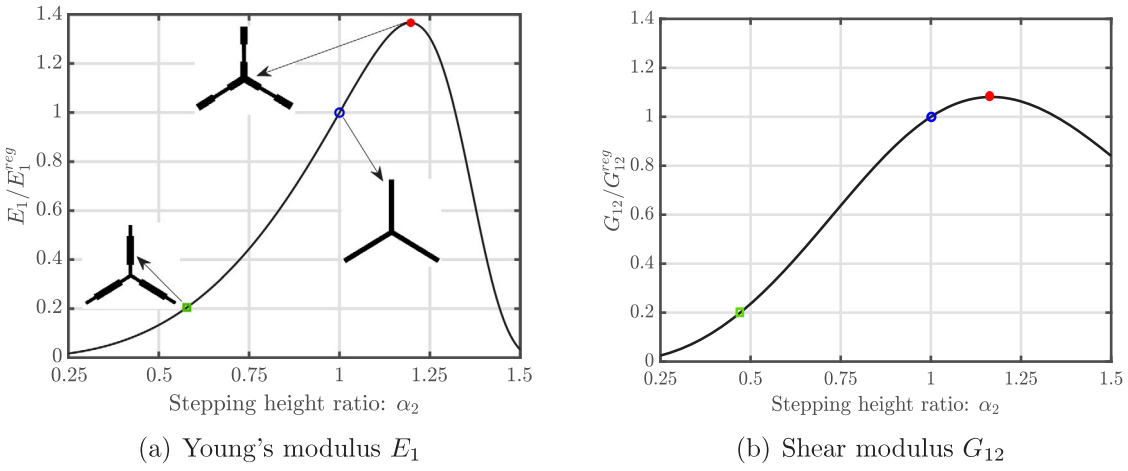

(a) Young's modulus E_1 (b) Shear modulus G_{12}

Fig. 17. Normalised (a) E_1 for different values of the stepping height ratio α_2. The optimum stepping length ratio is $\eta = 0.3195$ and (b) G_{12} for different values of the stepping height ratio α_2. The optimum stepping length ratio is $\eta = 0.1318$. The geometry of the corresponding unit cells are also shown for different regions. The red dots (a stepped-down lattice) shows the maximum value of normalised E_1 and G_{12} corresponding to the optimal value of α_2 in Eq. (128) and (134), respectively. The blue circle denotes the value corresponding to the regular lattice. The green square (a stepped-up lattice) denotes 80% lesser value of the normalised E_1 and G_{12} from the regular lattice. The height ratio is $\beta = h/L = 1$ and the cell angle is $\theta = 30°$.

For these values the G_{12} will obtain maximum value which is almost 8% higher than the regular case.

This study shows that there is a unique value of α_2 and η which gives the maximum value for E_1 and E_2. For G_{12} the values are different. We can observe that the optimum values of α_2 are close for both the cases but the η values differs a lot. It also shows that the material properties are sensitive to those geometric parameters. A small change in the thickness can substantially alter the property values. Results shown in Eq. (130) demonstrate that the equivalent elastic properties (E_1 and E_2) of an optimally designed hexagonal lattice are increased by almost 37% just by redistributing the mass of the constituent beam members through the geometric parameters given by Eqs. (128) and (129). The main focus in this present work consider the in-plane properties of the lattice. Apart from that, the hexagonal lattices are also used as a core material to increase the bending stiffness of sandwich structures. On the other hand, buckling of lattice metamaterials is an engaging topic and quite an open problem. There is a huge scope in this direction. The out of plane characteristics of lattice and analytical exploration considering buckling and large deformation are going to be investigated in our future works.

7. Conclusions

A generalised analytical framework to obtain the equivalent elastic properties of two-dimensional hexagonal lattices with arbitrary cross-sectional properties of the constituent beam members is proposed. Explicit closed-form expressions for the equivalent elastic properties of the stepped lattice are obtained. The stepped lattice is formed by redistributing the mass of the regular hexagonal lattice. This redistribution of mass results in increasing the design space compared to the lattices with regular constituent beam elements with a single cross-section. Unlike a conventional straight-beam lattice, the combined effect of the stepping length ratio (η) and the stepping height ratio (α_2) can be utilised simultaneously to tailor the required values of the equivalent elastic properties. The overall picture of the mass distribution, its effect on the equivalent Young's modulus and shear modulus and the corresponding shape of the unit cell (not to scale) is shown in Fig. 17. The plots are obtained for different values of stepping height ratio (α_2) and fixing the stepping length ratio to their optimum value, those are $\eta = 0.3195$ for the case of E_1 and $\eta = 0.1318$ for the case of G_{12}.

Some of the key novel features of this paper include:

- Two new types of hexagonal lattices, namely, stepped-up and stepped-down lattices, have been proposed. They are characterised by geometric parameters and have the same mass as the regular hexagonal lattice.
- Two approaches are combined with the unit cell method to obtain closed-form expressions for equivalent in-plane elastic properties of hexagonal lattices using the coefficients of the stiffness matrix of constituent stepped beams.
- Static condensation and the Castigliano method, along with the unit cell-based approach, are employed to obtain the equivalent elastic properties of the lattice. The static condensation-based approach can be utilised for constituent beam members with complex geometries. It is a semi-analytical method. Whereas, Castigliano method results in exact closed-form expressions for the elastic properties.
- Results show that by redistributing the mass of the constituent beam members of the lattice, both the stiffness and the flexibility can be enriched and altered in a prescribed manner. An optimum dimension for the constituent beam is also obtained to maximise the elastic moduli of the mass-conserved lattice. A vast range of equivalent material properties is demonstrated in this study which describes the enhanced design space.
- The optimised values of the parameters α_2 and η are different for Young's and Shear modulus. The value of α_2 is quite nearby for both the cases while η values are very much different. This shows a huge possibility of tuning, and tailoring of individual material parameters.
- A stepped-down lattice has a higher stiffness, whereas a stepped-up lattice has higher flexibility compared to an equivalent regular hexagonal lattice. An optimally designed stepped-down lattice can be up to 37% stiffer while keeping the mass almost the same as a regular lattice. For shear modulus the increasement is about 8.1%. This will lead to significant savings in materials and consequently reduced cost.

A closed-form solution for other lattices, such as auxetic, rhombus and rectangular geometries, have been explicitly derived as special cases of the general expressions proposed in the paper. The analytical expressions and the results obtained are benchmark results and can be directly used for the design of hexagonal lattices and other geometries. Future research directions will include exploring different mass conserved geometries and their non-linear dynamic analyses.

Declaration of competing interest

The authors declare that they have no known competing financial interests or personal relationships that could have appeared to influence the work reported in this paper.

Data availability

No data was used for the research described in the article.

References

[1] Frenzel T, Kadic M, Wegener M. Three-dimensional mechanical metamaterials with a twist. Science 2017;358(6366):1072–4.
[2] Wang K, Lin F, Chen J, Wei Z, Wei K, Yang X. Three-dimensional hierarchical metamaterials incorporating multi-directional programmable thermal expansion. Mech Mater 2021;163:104095.
[3] Wei K, Peng Y, Qu Z, Pei Y, Fang D. A cellular metastructure incorporating coupled negative thermal expansion and negative Poisson's ratio. Int J Solids Struct 2018;150:255–67.
[4] Chen J, Wang H, Wang K, Wei Z, Xu W, Wei K. Mechanical performances and coupling design for the mechanical metamaterials with tailorable thermal expansion. Mech Mater 2022;165:104176.
[5] Gibson L, Ashby MF. Cellular solids structure and properties. Cambridge, UK: Cambridge University Press; 1999.
[6] Fleck NA, Deshpande VS, Ashby MF. Micro-architectured materials: past, present and future. Proc R Soc A 2010;466(2121):2495–516.
[7] Cummer SA, Christensen J, Alù A. Controlling sound with acoustic metamaterials. Nat Rev Mater 2016;1(3):1–13.
[8] Hunt G, Dodwell T. Complexity in phase transforming pin-jointed auxetic lattices. Proc R Soc Lond Ser A Math Phys Eng Sci 2019;475(2224):20180720.
[9] Wang H, Zhao D, Jin Y, Wang M, Mukhopadhyay T, You Z. Modulation of multi-directional auxeticity in hybrid origami metamaterials. Appl Mater Today 2020;20:100715.
[10] Mukherjee S, Cajić M, Karličić D, Adhikari S. Enhancement of band-gap characteristics in hexagonal and re-entrant lattices via curved beams. Compos Struct 2023;306:116591.
[11] Wilbert A, Jang W-Y, Kyriakides S, Floccari J. Buckling and progressive crushing of laterally loaded honeycomb. Int J Solids Struct 2011;48(5):803–16.
[12] Sun J, Gao H, Scarpa F, Lira C, Liu Y, Leng J. Active inflatable auxetic honeycomb structural concept for morphing wingtips. Smart Mater Struct 2014;23(12):125023.
[13] Jang W-Y, Kyriakides S. On the buckling and crushing of expanded honeycomb. Int J Mech Sci 2015;91:81–90.
[14] Genoese A, Genoese A, Rizzi NL, Salerno G. Force constants of BN, SiC, AlN and GaN sheets through discrete homogenization. Meccanica 2018;53(3):593–611.
[15] Reda H, Alavi S, Nasimsobhan M, Ganghoffer J. Homogenization towards chiral Cosserat continua and applications to enhanced Timoshenko beam theories. Mech Mater 2021;155:103728.
[16] Alavi S, Ganghoffer J, Reda H, Sadighi M. Construction of micromorphic continua by homogenization based on variational principles. J Mech Phys Solids 2021;153:104278.
[17] Rizzi G, Dal Corso F, Veber D, Bigoni D. Identification of second-gradient elastic materials from planar hexagonal lattices. Part I: Analytical derivation of equivalent constitutive tensors. Int J Solids Struct 2019;176:1–18.
[18] Rizzi G, Dal Corso F, Veber D, Bigoni D. Identification of second-gradient elastic materials from planar hexagonal lattices. Part II: Mechanical characteristics and model validation. Int J Solids Struct 2019;176:19–35.
[19] Alavi S, Nasimsobhan M, Ganghoffer J, Sinoimeri A, Sadighi M. Chiral Cosserat model for architected materials constructed by homogenization. Meccanica 2021;56(10):2547–74.
[20] Alavi S, Ganghoffer J, Sadighi M, Nasimsobhan M, Akbarzadeh A. Continualization method of lattice materials and analysis of size effects revisited based on Cosserat models. Int J Solids Struct 2022;254:111894.
[21] Alavi SE, Ganghoffer J-F, Sadighi M. Chiral Cosserat homogenized constitutive models of architected media based on micromorphic homogenization. Math Mech Solids 2022;27(10):2287–313.
[22] Balawi S, Abot J. A refined model for the effective in-plane elastic moduli of hexagonal honeycombs. Compos Struct 2008;84(2):147–58.
[23] Niu B, Wang B. Directional mechanical properties and wave propagation directionality of Kagome honeycomb structures. Eur J Mech A Solids 2016;57:45–58.
[24] Adhikari S. The in-plane mechanical properties of highly compressible and stretchable 2D lattices. Compos Struct 2021;272:114167.
[25] Karakoç A, Santaoja K, Freund J. Simulation experiments on the effective in-plane compliance of the honeycomb materials. Compos Struct 2013;96:312–20.
[26] Baran T, Öztürk M. In-plane elasticity of a strengthened re-entrant honeycomb cell. Eur J Mech A Solids 2020;83:104037.
[27] Chen Q, Pugno NM. In-plane elastic buckling of hierarchical honeycomb materials. Eur J Mech A Solids 2012;34:120–9.
[28] Adhikari S. The eigenbuckling analysis of hexagonal lattices: Closed-form solutions. Proc R Soc Lond Ser A 2021;477(2251):20210244.
[29] Gasparetto VE, ElSayed MS. Shape transformers for phononic band gaps tuning in two-dimensional bloch-periodic lattice structures. Eur J Mech A Solids 2021;104278.
[30] Gibson L, Easterling K, Ashby MF. The structure and mechanics of cork. Proc R Soc Lond Ser A Math Phys Eng Sci 1981;377(1769):99–117.
[31] Rad MS, Prawoto Y, Ahmad Z. Analytical solution and finite element approach to the 3D re-entrant structures of auxetic materials. Mech Mater 2014;74:76–87.
[32] Mukhopadhyay T, Adhikari S. Effective in-plane elastic moduli of quasi-random spatially irregular hexagonal lattices. Internat J Engrg Sci 2017;119:142–79.
[33] Chen Y, Hu H. In-plane elasticity of regular hexagonal honeycombs with three different joints: A comparative study. Mech Mater 2020;148:103496.
[34] Li T, Hu X, Chen Y, Wang L. Harnessing out-of-plane deformation to design 3D architected lattice metamaterials with tunable Poisson's ratio. Sci Rep 2017;7(1):1–10.
[35] Jia Z, Liu F, Jiang X, Wang L. Engineering lattice metamaterials for extreme property, programmability, and multifunctionality. J Appl Phys 2020;127(15):150901.
[36] Masters IG, Evans KE. Models for the elastic deformation of honeycombs. Compos Struct 1996;35(4):403–22.
[37] Abd El-Sayed F, Jones R, Burgess I. A theoretical approach to the deformation of honeycomb based composite materials. Composites 1979;10(4):209–14.
[38] Zschernack C, Wadee MA, Völlmecke C. Nonlinear buckling of fibre-reinforced unit cells of lattice materials. Compos Struct 2016;136:217–28.
[39] Huang T, Gong Y, Zhao S. Effective in-plane elastic modulus of a periodic regular hexagonal honeycomb core with thick walls. J Eng Mech 2018;144(2):06017019.
[40] Bodaghi M, Damanpack A, Hu G, Liao W. Large deformations of soft metamaterials fabricated by 3D printing. Mater Des 2017;131:81–91.
[41] Weeger O, Boddeti N, Yeung S-K, Kaijima S, Dunn ML. Digital design and nonlinear simulation for additive manufacturing of soft lattice structures. Addit Manuf 2019;25:39–49.
[42] Jiang Y, Wang Q. Highly-stretchable 3D-architected mechanical metamaterials. Sci Rep 2016;6(1):1–11.
[43] Morin SA, Shepherd RF, Kwok SW, Stokes AA, Nemiroski A, Whitesides GM. Camouflage and display for soft machines. Science 2012;337(6096):828–32.
[44] Felton S, Tolley M, Demaine E, Rus D, Wood R. A method for building self-folding machines. Science 2014;345(6197):644–6.
[45] Restrepo D, Mankame ND, Zavattieri PD. Programmable materials based on periodic cellular solids. Part I: Experiments. Int J Solids Struct 2016;100:485–504.
[46] Mukherjee S, Adhikari S. A general analytical framework for the mechanics of heterogeneous hexagonal lattices. Thin-Walled Struct 2021;167:108188.
[47] Mukherjee S, Adhikari S. The in-plane mechanics of a family of curved 2D lattices. Compos Struct 2021;114859.
[48] Spears TG, Gold SA. In-process sensing in selective laser melting (SLM) additive manufacturing. Integr Mater Manuf Innov 2016;5(1):16–40.
[49] Korkmaz ME, Gupta MK, Robak G, Moj K, Krolczyk GM, Kuntoğlu M. Development of lattice structure with selective laser melting process: A state of the art on properties, future trends and challenges. J Manuf Process 2022;81:1040–63.
[50] Adhikari S, Mukhopadhyay T, Liu X. Broadband dynamic elastic moduli of honeycomb lattice materials: A generalized analytical approach. Mech Mater 2021;103796.
[51] Adhikari S. Exact transcendental stiffness matrices of general beam-columns embedded in elastic mediums. Comput Struct 2021;255(10):106617.
[52] Friedman Z, Kosmatka J. Exact stiffness matrix of a nonuniform beam—I. Extension, torsion, and bending of a Bernoulli–Euler beam. Comput Struct 1992;42(5):671–82.
[53] Friedman Z, Kosmatka J. Exact stiffness matrix of a nonuniform beam—II. Bending of a Timoshenko beam. Comput Struct 1993;49(3):545–55.
[54] Dawe D. Matrix and finite element displacement analysis of structures. Oxford, UK: Oxford University Press; 1984.
[55] Rao SS. Engineering optimization: Theory and practice. John Wiley & Sons; 2019.